Entropy Stable Hermite Approximation of the Linearised Boltzmann Equation for Inflow and Outflow Boundaries

Neeraj Sarna and Manuel Torrilhon

Center for Computational Engineering & Department of Mathematics
RWTH Aachen University, Germany*
(sarna@mathcces.rwth-aachen.de, mt@mathcces.rwth-aachen.de)

Abstract

To obtain a symmetric hyperbolic moment system from the linearised Boltzmann equation, we approximate the entropy variable (derivative of the entropy functional) with the help of multi-variate polynomials in the velocity space. Choosing the entropy functional to be quadratic, we retrieve the Grad's approximation for the linearised Boltzmann equation.

We develop a necessary and sufficient condition for the entropy stability of the Grad's approximation on bounded position domain with inflow and outflow boundaries. These conditions show the importance of using the *Onsager Boundary Conditions*(OBCs) (Physics of Fluids 28(2):027105, 2016) for obtaining entropy stability and we use them to prove that a broad class of Grad's approximations, equipped with boundary conditions obtained through continuity of odd fluxes (Commun Pure Appl Math 2(4):331407, 1949), are entropy unstable. Entropy stability, for the Grad's approximation, is obtained through entropy stabilization of the boundary conditions obtained through the continuity of odd fluxes. Since many practical implementations require the prescription of an inflow velocity, the entropy bounds for two possible methods to achieve the same is discussed in detail, both for the linearised Boltzmann equation and its Hermite approximation. We use the Discontinuous Galerkin (DG) discretization in the physical space, to study several benchmark problems to ascertain the physical accuracy of the proposed entropy stable Grad's approximation.

1 Introduction

A gas consists of molecules which move around in space with varying velocities and interact with each other through a well-defined interaction potential. The most intuitive way to study the evolution of a gas is with the help of molecular dynamics, in which every molecule is tracked both in space and time. Needles to say, due to the inherent high dimensionality, molecular dynamics, at macroscopic length scales, is a relatively expensive computational technique due to the presence of a large number of gas molecules. Therefore, instead of monitoring the motion of every individual particle, one concerns himself with the evolution of the so called phase density functional which significantly reduces the dimensionality of the problem. The evolution of the phase density functional, under certain assumptions, is given by the Boltzmann equation (BE); though cheap as compared to molecular dynamics, the Boltzmann equation is also high dimensional thus making a direct discretization of the Boltzmann equation expensive. In the recent decades, the Direct Simulation Monte Carlo (DSMC) method has proved to be a method of high fidelity for solving the BE; see [7] for an elaborate discussion.

Focusing on low Mach rarefied gas flows on bounded position domains, we are concerned with the linearised BE, which is scalar and hyperbolic in nature [10]. Due to the dissipation caused by the collision

*Mathematics (CCES), Schinkelstr. 2, 52062 Aachen, Germany

between the particles [10, 33], the a-priori entropy bound for the linearised BE is solely dependent upon the entropy flux across the boundary (or on the boundary conditions). The boundary conditions for the linearised BE trivially follow from its scalar hyperbolic nature and lead to its entropy stability under certain additional assumptions on the boundary data [18, 30]; an approximation for the linearised BE which preserves this entropy stability will then be an entropy stable approximation [38]. Since the velocity space is independent of the physical space, the first step towards approximating the linearised BE, in an entropy stable way, could be to formulate an entropy stable velocity space approximation which will be done with the help of moment approximations [33]. The entropy stability of a moment approximation cannot be underestimated since it can be used to ensure (i) its convergence to the solution of the Boltzmann equation as the number of moments are increased [30], (iii) the convergence of a further spatial discretization (specially on curved domains) [41] and (ii) the well-posedness of the initial boundary value problem (IBVP) resulting from the moment approximation [6].

The entropy stability of a moment approximation can be studied only if it is equipped with an entropy functional (or is symmetric hyperbolic). Using the framework developed in [21], to obtain a symmetric hyperbolic moment system, we approximate the entropy variable with the help of multi-variate polynomials in the velocity space. To obtain an explicit approximation for the phase density functional, with a polynomial approximation for the entropy variable, one requires to chose a suitable entropy functional; in the present work the entropy functional will be quadratic in nature [11]. Our choice of the entropy functional will lead to the Grad's approximation [8, 17, 39] for the phase density functional. This will further confirm the symmetric hyperbolicity of the linearised Grad's moment equations and will disclose an underling polynomial approximation for the entropy variable.

Similar to the linearised BE, the entropy stability of the moment approximation also depends upon a well defined set of boundary conditions [28, 31] (a similar statement for the Euler and the Navier-Stokes equations, which are a particular type of moment approximations, also holds true [25–27, 37]). We will prove that a necessary and sufficient condition for the entropy stability, of the moment approximation, is the use of *Onsager Boundary Conditions* (OBCs), which are given in terms of an unknown *Onsager matrix*. Since the boundary conditions proposed by Grad[17] have the same structure as the OBCs [31], we will first prove that they lead to entropy instabilities and then, similar to [28, 31, 34], will use them to construct a model for the *Onsager matrix*.

We will study the entropy bounds for two possible methodologies to prescribe a particular inflow velocity. The first methodology will rely on altering the incoming distribution only along the inflow boundary such that the desired inflow velocity is reached. The second methodology will rely on prescribing a given incoming distribution function (which will be independent of the solution) and changing the boundary conditions along both the inflow and outflow boundaries in an iterative way to obtain the desired inflow velocity. The second methodology, of the two, will be shown to be entropy stable and an entropy stabilization technique will be proposed for the first methodology. The accuracy of the proposed stabilisation will be studied with a benchmark problem.

2 The Boltzmann Equation

Let $(t,\mathbf{x},\xi) \in (0,T] \times \Omega \times \mathbb{R}^d$, where we will assume $\Omega \subseteq \mathbb{R}^d$ to be smooth and convex. Let $\bar{f} : (0,T] \times \Omega \times \mathbb{R}^d \to \mathbb{R}^+$, $(t,\mathbf{x},\xi) \mapsto \bar{f}(t,\mathbf{x},\xi)$, denote the phase density functional of a gas. With the help of $\bar{f}$, the density (ρ), velocity(v_i) and temperature (θ) of the gas can be defined: $\rho = \int_{\mathbb{R}^d} \bar{f} d\xi$, $\rho v_i = \int_{\mathbb{R}^d} \xi_i \bar{f} d\xi$ and $\rho v_i v_i + d\rho\theta = \int_{\mathbb{R}^d} \xi_i \xi_i \bar{f} d\xi$. To study low Mach gas flows, we will assume $\bar{f}$ to be a small perturbation of the ground state [39]

$$f_0 = \frac{\rho_0}{\left(\sqrt{2\pi\theta_0}\right)^d} \exp\left(-\frac{\xi_i \xi_i}{2\theta_0}\right) \tag{1}$$

i.e. $\bar{f} = f_0 + \varepsilon f$ with ε being some smallness parameter. In (1), ρ_0 and θ_0 represent some constant ground states of ρ and θ respectively. The governing equation for f can then be given as [39]

$$\partial_t f + \xi_i \partial_{x_i} f = Q(f), \quad \text{in} \quad (0,T] \times \Omega \times \mathbb{R}^d, \tag{2}$$

the initial and the boundary conditions for which will be discussed later. The linearised collision operator $Q(f)$ can be obtained by linearising the Boltzmann collision operator about f_0 and is given as [10]

$$Q(f) = \int_{\mathbb{R}^3} \int_{S^2_+} \sigma(\xi - \xi_1, \kappa) \tag{3}$$

$$\times f_0(\xi_1) f_0(\xi) \left(\frac{f(\xi')}{f_0(\xi')} + \frac{f(\xi_1')}{f_0(\xi_1')} - \frac{f(\xi_1)}{f_0(\xi_1)} - \frac{f(\xi)}{f_0(\xi)} \right) d\kappa d\xi_1, \quad f \in \mathscr{D}(Q) \tag{4}$$

where ξ_1' and ξ' are the post collisional velocities and are defined as $\xi' = \xi - [(\xi - \xi_1).\kappa]\kappa$, $\xi_1' = \xi_1 - [(\xi_1 - \xi).\kappa]\kappa$, σ is the collision kernel which changes with the type of interaction potential being used and $\mathscr{D}(Q)$ is the domain of the collision operator Q. The linearised collision operator $Q(f)$ vanishes if and only if $f = f_{\mathscr{M}}$ with

$$f_{\mathscr{M}}(\xi; \tilde{\rho}, \tilde{\mathbf{v}}, \tilde{\theta}) = \left(\frac{\tilde{\rho}}{\rho_0} + \frac{\tilde{v}_i \xi_i}{\theta_0} + \frac{\tilde{\theta}}{2\theta_0} \left(\frac{\xi_i \xi_i}{\theta_0} - 3 \right) \right) f_0(\xi) \tag{5}$$

where $\tilde{\rho}$, $\tilde{v}_i$ and $\tilde{\theta}$ represent the deviation of ρ, v_i and θ from their respective ground states (ρ_0, $\mathbf{0}$ and θ_0 respectively) upto $\mathscr{O}(\varepsilon)$. Every element of $\mathscr{I} = \{1, \xi_i, \xi_i \xi_i\}$ is a collision invariant of $Q(f)$ [10]

$$\int_{\mathbb{R}^d} v Q(f) d\xi = 0, \quad \forall (v, f) \in \mathscr{I} \times \mathscr{D}(Q). \tag{6}$$

Due to (6), multiplying the linearised BE by any element of $\mathscr{I}$ and integrating over the entire velocity space, it follows that the linearised BE conserves mass, momentum and energy and mimics the conservation of these quantities during the binary collision of two mono-atomic gas molecules. Moreover, the linearised BE is Galilean invariant i.e for any arbitrary velocity $\mathbf{U} \in \mathbb{R}^d$ and an orthogonal matrix $\mathbf{O} \in \mathbb{R}^{d \times d}$, if $f(t, \mathbf{x}, \xi)$ is a solution to the linearised BE then so is $f(t, \mathbf{x} - \mathbf{U}t, \xi - \mathbf{U})$ and $f(\mathbf{O}^T \mathbf{x}, \mathbf{O}^T \xi, t)$ [10]. For convenience we introduce the Hilbert space $\mathscr{H} = L^2(\mathbb{R}^d, f_0^{-1})$ with the corresponding inner product $\langle ., . \rangle_{\mathscr{H}}$ and the norm $\|.\|_{\mathscr{H}}$.

2.1 Initial and Boundary Conditions

The initial conditions can be prescribed through the relation

$$f(t = 0, \mathbf{x}, \xi) = f_I(\mathbf{x}, \xi), \quad \text{in} \quad \Omega \times \mathbb{R}^d \tag{7}$$

where we will assume $f_I(., \xi) \in C^1(\Omega) \forall \xi \in \mathbb{R}^d$ and $f_I(\mathbf{x}, \xi) \in L^2(\Omega; \mathscr{H})$. Let $\partial\Omega$ be a smooth boundary of the domain Ω, with $\mathbf{n}(\mathbf{x})$ being a unit vector which points out of the domain and is perpendicular to $\partial\Omega$ at $\mathbf{x}$. Due to the hyperbolic nature of the linearised BE, at a particular point at the boundary, we need to prescribe a value to that part of the distribution function which corresponds to $\xi_i n_i = \xi_n < 0$ (i.e the

distribution function of those particles which come into the domain). Thus, microscopically, the inflow (or the outflow) boundary conditions can be prescribed as [30]

$$f(t,\mathbf{x},\xi) = f_{in}(t,\mathbf{x},\xi), \quad \text{in} \quad (0,T]\times\partial\Omega\times\mathbb{R}^d_-. \tag{8}$$

where $\mathbb{R}^d_-$ is the set of all $\xi\in\mathbb{R}^d$ such that $\xi_n<0$. We will assume f_{in}, without any loss of generality, to be given by

$$f_{in}(t,\mathbf{x},\xi) = f_{\mathscr{M}}(\xi;\tilde{\rho}_{in}(t,\mathbf{x}),\mathbf{0},\tilde{\theta}_{in}(t,\mathbf{x})), \tag{9}$$

where $\tilde{\rho}_{in}$ and $\tilde{\theta}_{in}$ are smooth functions along the boundary and could either be given or can be computed such that the boundary conditions satisfy certain constraints; for e.g. at the gas-wall interface, $\tilde{\rho}_{in}$ is computed such that the relative velocity of the gas normal to the wall remains zero [10, 33].

Let $\partial\Omega=\partial\Omega^+\cup\partial\Omega^-$ with $\partial\Omega^+$ and $\partial\Omega^-$ being non-overlapping. Let the normal velocity $\tilde{v}_i n_i$ along $\partial\Omega^+$ and $\partial\Omega^-$ be negative and positive respectively. Then, $\partial\Omega^+$ will correspond to the inflow boundary and $\partial\Omega^-$ will correspond to the outflow boundary. We can relate the definitions of the microscopic boundary conditions in (8) with our definitions of the inflow and the outflow boundaries in the following way. Let $f^+_{in}(\mathbf{x},\xi,t)=f_{\mathscr{M}}(\xi;\tilde{\rho}^+(\mathbf{x},t),\mathbf{0},\tilde{\theta}^+(\mathbf{x},t))$ and $f^-_{in}(\mathbf{x},\xi,t)=\tilde{f}_{\mathscr{M}}(\xi;\tilde{\rho}^-(\mathbf{x},t),\mathbf{0},\tilde{\theta}^-(\mathbf{x},t))$ represent the incoming distribution function along $\partial\Omega^+$ and $\partial\Omega^-$ respectively. In order to ensure a negative and a positive normal velocity along $\partial\Omega^+$ and $\partial\Omega^-$ respectively, the parameters $\tilde{\rho}^{(\pm)}$ and $\tilde{\theta}^{(\pm)}$ should be chosen appropriately. We will assume that such a normal velocity can be ensured by choosing a $\tilde{\rho}_{in}$ and $\tilde{\theta}_{in}$ such that the deviation in pressure upto $\mathscr{O}(\varepsilon)$, $\tilde{\rho}\theta_0+\tilde{\theta}\rho_0$, corresponding to the incoming distribution function along $\partial\Omega^+$ is higher as compared to the pressure of the incoming distribution function along $\partial\Omega^-$ i.e $\tilde{\rho}^+\theta_0+\tilde{\theta}^+\rho_0>\tilde{\rho}^-\theta_0+\tilde{\theta}^-\rho_0$. Thus leading to a net pressure driven flow from $\partial\Omega^+$ to $\partial\Omega^-$ which makes them the inflow and the outflow boundaries respectively.

Remark 1. There might be physical situations such that even after ensuring $\theta_0\tilde{\rho}^+ + \rho_0\tilde{\theta}^+ > \theta_0\tilde{\rho}^- + \rho_0\tilde{\theta}^-$, we might not obtain a net pressure driven flow from $\partial\Omega^+$ to $\partial\Omega^-$. But our assumption of $\theta_0\tilde{\rho}^+ + \rho_0\tilde{\theta}^+$ being greater than $\theta_0\tilde{\rho}^- + \rho_0\tilde{\theta}^-$ is simply for the sake of definition and it does not put any restriction upon the framework to be developed in the coming discussion.

Remark 2. For further discussion we will assume that there exists a strong solution to the kinetic IBVP ((2), (8) and (7)) i.e. $f(.,.,\xi)\in C^1((0,T]\times\Omega)\forall\xi\in\mathbb{R}^d$; the uniqueness of the solution will be clear from the entropy stability to be discussed later.

2.2 Entropy Functional

Entropy Dissipation: Let $\eta:\mathscr{D}(Q)\to\mathbb{R}$, $f\mapsto\eta(f)$, be a strictly convex entropy functional of the linearised BE then, for all $f\in\mathscr{D}(Q)$, it holds [10]

$$\int_{\mathbb{R}^d}\partial_f\eta(f)Q(f)d\xi\le 0 \tag{10}$$

Defining the entropy flux, $\phi^{(i)}(f)$, as

$$\partial_f\phi^{(i)}(f)=\xi_i\partial_f\eta(f), \tag{11}$$

we can multiply the linearised BE by $\partial_f\eta(f)$ and integrate over the entire velocity space to obtain the entropy dissipation law

$$\partial_t \int_{\mathbb{R}^d} \eta d\xi + \partial_{x_i} \int_{\mathbb{R}^d} \phi^{(i)} d\xi = \int_{\mathbb{R}^d} \partial_f \eta(f) Q(f) d\xi \leq 0 \tag{12}$$

It is clear from (12) that in a spatially homogeneous physical situation, the dissipation of the entropy functional caused by collision between particles (10), ensures that $\int_{\mathbb{R}^d} \eta d\xi$ decays continuously in time. At steady state, $\int_{\mathbb{R}^d} \eta d\xi$ will be minimum which is equivalent to requiring the equality in (10), which is further equivalent to requiring $f = f_{\mathscr{M}}$ [33]. Thus, the entropy dissipation law (12) can be looked upon as an abstraction of the H-theorem.

Remark 3. The conclusion that $\int_{\mathbb{R}^d} \eta d\xi$ is minimised, in steady state, for a given physical process is necessarily true only for spatially homogeneous flows. For spatially inhomogeneous flows, involving bounded position domains, the entropy flux across the boundary can lead to a bounded growth in $\int_{\mathbb{R}^d} \eta d\xi$, though the dissipation caused by the collisions (10) will remain negative.

Entropic Reformulation of the Linearised BE : Let the entropy variable (h) and the mapping relating the entropy variable to f, ($h \mapsto \mathscr{F}(h)$), corresponding to the linearised BE (2), be defined as

$$h = \partial_f \eta(f), \quad f = \mathscr{F}(h) \quad \text{where } \mathscr{F} = (\partial_f \eta)^{-1}. \tag{13}$$

Note that $\partial_f \eta$ is a one to one mapping and hence invertible [19]. Expressing f in terms of the entropy variable, (2) can be reformulated as

$$\partial_t \mathscr{F}(h) + \xi_i \partial_{x_i} \mathscr{F}(h) = Q(\mathscr{F}(h)). \tag{14}$$

Since (14) can be looked upon as an evolution equation for the entropy variable, we will call (14) the entropic reformulation of the linearised BE.

The entropic reformulation will provide us with a generic framework to develop symmetric hyperbolic moment systems [21]. Multiplying (14) by h and integrating over the velocity space, we immediately recover the entropy dissipation law (12) due to (10). Thus, the entropic reformulation will provide an easier access towards entropy estimates for the moment systems.

2.3 Symmetric Hyperbolic Moment Approximation

In order to approximate the solution to our IBVP ((2), (8) and (7)), we will take the help of moment approximations. To define the notion of moments, similar to [8, 17], we define a set $\mathscr{V}_M$ which contains all the tensorial Hermite polynomials ($\psi_{\beta^{(i)}}$) upto a certain degree

$$\begin{gathered}\psi_{\beta^{(i)}}(\xi) = \prod_{p=1}^{d} He_{m_p^{(i)}}\left(\frac{\xi_p}{\sqrt{\theta_0}}\right), \quad \beta^{(i)} = \left(m_1^{(i)}, \ldots, m_d^{(i)}\right), \quad |\beta^{(i)}| = \sum_{p=1}^{d} m_p^{(i)} \leq M \\ \mathscr{V}_M = \{\psi_{\beta^{(i)}}\}_{|\beta^{(i)}| \leq M}\end{gathered} \tag{15}$$

with $\beta^{(i)}$ being a d-dimensional multi-index, $M \in \mathbb{N}$ and $|.|$ denoting the l^1 norm. The Hermite polynomials ($He_k(\xi)$) enjoy orthogonality and recursion

$$\int_{\mathbb{R}} He_i(\xi) He_j(\xi) \exp\left(-\frac{\xi^2}{2}\right) d\xi = \sqrt{2\pi}\delta_{ij} \tag{16a}$$

$$\sqrt{i+1} He_{i+1}(\xi) + \sqrt{i} He_{i-1}(\xi) = \xi He_i(\xi). \tag{16b}$$

Due to (16a), the tensorial Hermite polynomials are also orthogonal

$$\left\langle \psi_{\beta^{(k)}} f_0, \psi_{\beta^{(l)}} f_0 \right\rangle_{\mathscr{H}} = \rho_0 \prod_{p=1}^{d} \delta_{m_p^{(k)} m_p^{(l)}}. \tag{17}$$

Let $g : (t,\mathbf{x},\xi) \to \mathbb{R}$, $(t,\mathbf{x},\xi) \mapsto g(t,\mathbf{x},\xi)$, be any arbitrary functional such that $\psi_{\beta^{(i)}}(.)g(t,\mathbf{x},.) \in L^1(\mathbb{R}^d)$ for all $|\beta^{(i)}| \leq M$. Then a moment of $|\beta^{(i)}|^{th}$ order of g, $\mu_{\beta^{(i)}}(g)$, is defined as

$$\mu_{\beta^{(i)}}(g) = \int_{\mathbb{R}^d} \psi_{\beta^{(i)}} g d\xi, \quad |\beta^{(i)}| \leq M. \tag{18}$$

For a moment approximation of the linearised BE, we will concern ourselves with the evolution of $\mu_{\beta^{(i)}}(f)$. In order to find the governing equations for $\mu_{\beta^{(i)}}(f)$, we multiply the linearised BE (2) and the initial conditions (7) by all the elements of $span(\mathscr{V}_M)$ and integrate over the velocity space to obtain

$$\begin{gathered} \int_{\mathbb{R}^d} v\partial_t \mathscr{F}(h) d\xi + \int_{\mathbb{R}^d} v\xi_i \partial_{x_i} \mathscr{F}(h) d\xi = \int_{\mathbb{R}^d} vQ(\mathscr{F}(h)) d\xi \quad \forall v \in span(\mathscr{V}_M) \\ \mu_{\beta^{(i)}}(f(t=0,\mathbf{x},\xi)) = \mu_{\beta^{(i)}}(f_I(\mathbf{x},\xi)) \end{gathered} \tag{19}$$

We have implicitly assumed that the true solution is such that all the integrals in (19) exist i.e. $\mathscr{F}(h) \in \mathbb{S}$ where

$$\begin{aligned} \mathbb{S} = \Big\{ & \mathscr{F}(h) \in \mathscr{D}(Q) : v\mathscr{F}(h) \in L^1(\mathbb{R}^d), \quad \xi v \mathscr{F}(h) \in \left[L^1(\mathbb{R}^d)\right]^d, \\ & vQ(\mathscr{F}(h)) \in L^1(\mathbb{R}^d) \quad \forall v \in span(\mathscr{V}_M) \Big\} \end{aligned} \tag{20}$$

Therefore for the mere formulation of the moment system, we need some additional regularity on the exact solution. By choosing v to be the different elements of $\mathscr{V}_M$ in (19), one can arrive at a set of moment equations which govern the time evolution of $\mu_{\beta^{(i)}}(f)$ and are not closed (presence of a higher order moment in the fluxes) [33] . Therefore, to close the system in (19), we can approximate h by h_M such that h_M satisfies (19)

$$\begin{gathered} \int_{\mathbb{R}^d} v\partial_t \mathscr{F}(h_M) d\xi + \int_{\mathbb{R}^d} v\xi_i \partial_{x_i} \mathscr{F}(h_M) d\xi = \int_{\mathbb{R}^d} vQ(\mathscr{F}(h_M)) d\xi \quad \forall v \in span(\mathscr{V}_M) \\ \mu_{\beta^{(i)}}(\mathscr{F}(h_M(t=0,\mathbf{x},\xi))) = \mu_{\beta^{(i)}}(f_I(\mathbf{x},\xi)). \end{gathered} \tag{21}$$

By choosing v to be the different elements of $\mathscr{V}_M$ in (21), we can obtain a closed set of equations governing the evolution of $\mu_{\beta^{(i)}}(\mathscr{F}(h_M))$ which are some approximation to $\mu_{\beta^{(i)}}(f)$. A set of boundary conditions for the moment system (21) will be discussed later.

The closed moment system (21) should be such that it preserves the following properties of the linearised BE (i) mass, momentum and energy conservation, (ii) Galilean invariance and (iii) the existence of an entropy functional (or symmetric hyperbolicity). The reason behind requiring (iii) will become clear in the coming discussion, the reason for requiring the other two is self explanatory. The first requirement can be met by choosing $M \geq 2$ ($\mathscr{I} \subseteq \mathscr{V}_M$), whereas the second requirement is satisfied by the structure of the tensorial Hermite polynomials $\psi_{\beta^{(i)}}$ [40]. To ensure symmetric hyperbolicity, it is sufficient to express h_M as [21]

$$h_M(\mathbf{x},\xi,t) = \sum_{|\beta^{(i)}| \leq M} \alpha_{\beta^{(i)}}(\mathbf{x},t) \psi_{\beta^{(i)}}(\xi) \tag{22}$$

where $\alpha_{\beta^{(i)}}$ are some expansion coefficients and $\beta^{(i)}$ are the multi-indices as defined in (15). Note that (22) implies $h_M \in span\mathscr{V}_M$.

Remark 4. Ensuring (22) allows us to choose $v = h_M$ in (21), leading to

$$\partial_t \int_{\mathbb{R}^d} \eta(\mathscr{F}(h_M))d\xi + \partial_{x_i} \int_{\mathbb{R}^d} \phi^{(i)}(\mathscr{F}(h_M))d\xi = \int_{\mathbb{R}^d} \partial_f \eta(\mathscr{F}(h_M))Q(\mathscr{F}(h_M))d\xi \leq 0 \tag{23}$$

which is an approximation of the entropy dissipation law in (12). The existence of an entropy law implies that the moment system resulting from (21) will be symmetric hyperbolic [19].

For the discussion which follows, we will choose the entropy functional to be

$$\eta(f) = \frac{1}{2} f^2 f_0^{-1} \quad \Rightarrow \quad h = f f_0^{-1}, \quad \mathscr{F}(h) = h f_0. \tag{24}$$

The polynomial approximation for h_M (22) then implies

$$f \approx f_M = \mathscr{F}(h_M) = \sum_{|\beta^{(i)}| \leq M} \alpha_{\beta^{(i)}}(\mathbf{x},t)\psi_{\beta^{(i)}}(\xi) f_0. \tag{25}$$

which is the same as the Grad's approximation for the linearised BE. Note that an f_M given by the above expression belongs to $\mathbb{S}$, which is crucial for the existence of the integrals in (21). Moreover, due the the orthogonality of the basis functions the expansion coefficients are nothing but the moments of f_M i.e. $\rho_0 \alpha_{\beta^{(i)}} = \mu_{\beta^{(i)}}(f_M)$. For convenience we define the projector operator $\Pi_M : \mathscr{H} \to \mathscr{H}_M := span\{\psi_{\beta^{(i)}} f_0\}_{|\beta^{(i)}| \leq M}$ for any arbitrary $g \in \mathscr{H}$ as

$$\Pi_M(g) = \sum_{|\beta^{(i)}| \leq M} \left\langle \psi_{\beta^{(i)}} f_0, g \right\rangle_{\mathscr{H}} \psi_{\beta^{(i)}} f_0. \tag{26}$$

We now show that the choice to approximate the entropy variable, with the help of polynomials, also results from a special choice of the *re-normalisation map* hence, the variational formulation presented in (21) can also be interpreted as a special case of the variational formulation resulting from *re-normalisation* [3].

Relation to the renormalization map: Let $\mathscr{B} : span(\mathscr{V}_M) \to \mathbb{S}$ denote a so called *re-normalisation map*. The problem of finding a closure relation for the deviation in phase density functional, such that the moment system in (19) is closed, is then equivalent to explicitly defining a re-normalisation map i.e. we would like to have an approximation $\mathscr{F}(h) \approx \mathscr{B}(g_M)$, where $g_M \in span(\mathscr{V}_M)$, for some given $\mathscr{B}$. Approximating $\mathscr{F}(h)$ through $\mathscr{B}(g_M)$ in (19), the vartional form (21) can be recast as a Galerkin subspace projection [3]

$$\begin{aligned} &\text{Find } g_M \in span(\mathscr{V}_M) \text{ such that} \\ &\int_{\mathbb{R}^d} v\partial_t \mathscr{B}(g_M)d\xi + \int_{\mathbb{R}^d} v\xi_i \partial_{x_i} \mathscr{B}(g_M)d\xi = \int_{\mathbb{R}^d} vQ(\mathscr{B}(g_M))d\xi \quad \forall v \in span(\mathscr{V}_M). \end{aligned} \tag{27}$$

By appropriately choosing the *re-normalisation map*, both the Grad's [17] and the minimum entropy moment closure [21] can be easily recovered as a special case of (27) [3]. Choosing $\mathscr{B}$ to be the same as $\mathscr{F}$, we obtain

$$h_M = \mathscr{F}^{-1}\mathscr{F}(g_M) = g_M \quad \Rightarrow \quad h_M \in span(\mathscr{V}_M) \tag{28}$$

which is the same as expressing h_M through (22).

Remark 5. When the flow reaches local equilibrium, the following statements are equivalent [10]

$$\int_{\mathbb{R}^d} hQ(\mathscr{F}(h))d\xi = 0 \quad \Leftrightarrow \quad h \in span(\mathscr{I}) \quad \Leftrightarrow \quad f = f_{\mathscr{M}}. \tag{29}$$

Therefore, by choosing $M \geq 2$ in (22), the equilibrium state is contained in the approximation.

Remark 6. For all the coming discussion, we will be using $H(t)$ to denote a known bounded function of time. Usually, this function will contain contribution from boundary and initial data. New known factors might be included in $H(t)$ without changing the notation.

3 Entropy Stability

The entropy dissipation law (12) governs the evolution of $\int_{\mathbb{R}^d} \eta(f) d\xi$. In the present section, we would like to know how the entropy in the entire domain, i.e. $S(f) = \int_\Omega \int_{\mathbb{R}^d} \eta(f) d\xi d\mathbf{x}$, behaves. To obtain a governing equation for $S(f)$, we integrate the dissipation law in (12) over Ω and use the *Gauss-Theorem* to obtain

$$d_t S \leq -\int_{\partial\Omega} \int_{\mathbb{R}^d} n_i \phi^{(i)} d\xi ds, \tag{30}$$

where ds is the surface element along $\partial\Omega$ and n_i is a unit vector pointing out of the domain. The IBVP((2), (8) and (7)) will be entropy stable if we can show that $d_t S \leq H(t)$; such a bound on $S(f)$ requires appropriately defining the boundary conditions. Similarly, if we can ensure that the polynomial approximation to h (22) preserves a similar type of bound for $S(\mathscr{F}(h_M))$, i.e. $d_t S(\mathscr{F}(h_M)) \leq H(t)$, then we will obtain an entropy stable approximation for the linearised BE.

3.1 Entropy Bounds

The linearised BE: Using our choice of $\eta(f)$ from (24) and the definition of the entropy flux in (11), we obtain

$$\phi^{(i)}(f) = \frac{1}{2} \xi_i f^2 f_0^{-1}. \tag{31}$$

Since we have assumed f to be the strong solution of our kinetic IBVP, its value on the boundary is well defined. As a result, we can replace the boundary conditions for the linearised BE (8) into the entropy flux, leading to the simplification (recall $\xi_n = \xi_i n_i$)

$$\oint_{\partial\Omega} \int_{\mathbb{R}^d} \phi^{(i)} n_i d\xi ds = \frac{1}{2} \left[\oint_{\partial\Omega} \int_{\mathbb{R}^{d-1}} \int_{\xi_n \geq 0} \xi_n f^2 f_0^{-1} d\xi ds + \oint_{\partial\Omega} \int_{\mathbb{R}^{d-1}} \int_{\xi_n < 0} \xi_n f_{in}^2 f_0^{-1} d\xi ds \right] \tag{32}$$

For the chosen entropy functional, the flux of entropy which is carried by the molecules which move out of the domain, i.e. molecules with velocities $\xi_n \geq 0$, does not contribute into any entropy growth because $\int_{\mathbb{R}^{d-1}} \int_{\xi_n > 0} \xi_n f^2 f_0^{-1} d\xi > 0$. If we now consider $\tilde{\rho}^{in}$ and $\tilde{\theta}^{in}$ (9) to be given bounded functions of $\mathbf{x}$ and t (i.e. independent of the solution) then, the entropy flux corresponding to f_{in} can be assumed to be bounded as

$$-\oint_{\partial\Omega} \int_{\mathbb{R}^{d-1}} \int_{\xi_n < 0} \xi_n f_{in}^2 f_0^{-1} d\xi ds \leq H(t) \quad \Rightarrow \quad -\oint_{\partial\Omega} \int_{\mathbb{R}^d} \xi_n f^2 f_0^{-1} d\xi ds \leq H(t) \tag{33}$$

Using (33) in (30), we obtain

$$d_t S(f) \leq H(t) \tag{34}$$

Thus $S(f)$ is bounded independently of the solution which shows the entropy stability of the linearised BE for the chosen entropy functional.

Remark 7. The fact that we can bound the entropy flux corresponding to the positive and the negative ξ_n independently, is a consequence of $\phi^{(i)}$ having the same sign as ξ_n which is a result of the positivity of the entropy functional given in (24). For any other choice of the entropy functional, as described in [12], one might have to modify $\eta(f)$ to $\bar{\eta}(f)$ such that $\bar{\eta}(f)$ remains a valid entropy functional for the linearised BE and is positive. This methodology has been used to study the entropy stability of the Navier-Stokes equations in [12, 36] but it is presently unclear as to how it can be used for the linear (or the non-linear) BE on bounded position domains.

Remark 8. Integrating the estimate in (30) over time we find that $f \in C^0((0,T];L^2(\Omega;\mathscr{H}))$. Since the tensorial Hermite polynomials form a complete set of basis in $L^2(\mathbb{R}^d, f_0)$ [16], we can represent the solution to the kinetic equation as

$$f(t,\mathbf{x},\xi) = \lim_{M\to\infty} \sum_{|\beta^{(i)}|\leq M} \alpha^{(BE)}_{\beta^{(i)}}(t,\mathbf{x})\psi_{\beta^{(i)}}(\xi)f_0(\xi), \tag{35}$$

where, due to the assumption of a strong solution, $\alpha^{(BE)}_{\beta^{(i)}} \in C^1((0,T]\times\Omega)$ and are related to the moments of f as $\rho_0\alpha^{(BE)}_{\beta^{(i)}} = \mu_{\beta^{(i)}}(f)$.

The moment approximation : Integrating the entropy dissipation law in (23) over the entire domain Ω and using *Gauss-Theorem* we obtain

$$d_t S(f_M) + \int_{\partial\Omega}\int_{\mathbb{R}^d} \phi^{(i)}(f_M) n_i d\xi ds \leq 0 \tag{36}$$

where f_M is given by (25) and

$$S(f_M) = \int_\Omega \int_{\mathbb{R}^d} \frac{1}{2} f_M^2 f_0^{-1} d\xi d\mathbf{x}, \quad \phi^{(i)}(f_M) = \frac{1}{2}\xi_i f_M^2 f_0^{-1}. \tag{37}$$

Similar to (33), bounding the entropy flux in (36) in terms of $H(t)$ will ensure the entropy stability of the approximation (22). Hence, we require

$$-\oint_{\partial\Omega}\int_{\mathbb{R}^d} \phi^{(i)}(f_M) n_i d\xi ds \leq H(t). \tag{38}$$

Using (38) in (36) provides

$$d_t S(f_M) \leq H(t), \tag{39}$$

which is similar to (34) and leads to entropy stability of the approximation. We will now formulate necessary and sufficient conditions under which the inequality in (38) is satisfied which will also provide us with a generic set of boundary conditions for the moment approximation (21). For all the coming discussion we will assume $\tilde{\rho}_{in}$ and $\tilde{\theta}_{in}$ to be independent of the solution unless otherwise mentioned.

Remark 9. The approximation f_M is continuous in the entire velocity space. Therefore contrary to (33), we cannot split the velocity space integral in (38) into two parts, one each over a positive and a negative ξ_n, and bound them independently. Neither it is clear how to use the discrete velocity boundary conditions for the approximation (25) in case $d > 1$ [31]. Hence, to obtain entropy stability, we will try to bound the integral over the entire velocity space in (38) with the help of $H(t)$.

Remark 10. Using the orthogonality of the Hermite polynomials (16a), we find

$$S(f_M) = \sum_{|\beta^{(i)}|\leq M} \int_\Omega \frac{(\alpha_{\beta^{(i)}})^2}{2} d\mathbf{x}. \tag{40}$$

Therefore, if we can provide the moment approximation (21) with the correct number of boundary conditions and ensure a bound of the type (39) then it can be easily shown, with the framework developed in [6, 25], that the linear IBVP resulting from our moment approximation (21) will be well-posed.

3.2 Necessary and Sufficient Condition for Entropy Stability

For simplicity we will assume that the domain is cubic, $\Omega = [0,1]\times[0,1]\times[0,1]$, with a boundary surface that does not contribute into any growth of the entropy apart from the face at $x_1 = 1$; we will denote this face by $\partial\Omega_1$. This simplifies (38) to

$$-\int_{\partial\Omega_1}\int_{\mathbb{R}^d} \phi^{(1)}(f_M) d\xi ds \leq H(t). \tag{41}$$

A brief discussion on extending the following results to curved boundaries can be found in subsubsection 3.4. The entropy flux in (41) can be further simplified by splitting f_M as $f_M = f_M^o + f_M^e$ where f_M^o and f_M^e are the even and the odd parts of f_M, with respect to ξ_1, respectively and can be expressed as

$$f_M^o = \sum_{|\beta^{(i,o)}|\leq M} \alpha_{\beta^{(i,o)}} \psi_{\beta^{(i,o)}} f_0, \quad f_M^e = \sum_{|\beta^{(i,e)}|\leq M} \alpha_{\beta^{(i,e)}} \psi_{\beta^{(i,e)}} f_0 \tag{42}$$

where $\psi_{\beta^{(i,o)}}$ and $\psi_{\beta^{(i,e)}}$ are those basis functions, out of all the basis functions $\psi_{\beta^{(i)}}$, which are odd and even in ξ_1 respectively; see subsection 8.1 for an example showing the multi-indices $\beta^{(i)}$, $\beta^{(i,o)}$ and $\beta^{(i,e)}$ corresponding to $M = 3$. The coefficients $\alpha_{\beta^{(i,o)}}$ and $\alpha_{\beta^{(i,e)}}$ are the odd and even moments of f_M respectively and can be given as

$$\rho_0 \alpha_{\beta^{(i,e)}} = \left\langle f_M^e, \psi_{\beta^{(i,e)}} f_0 \right\rangle_{\mathscr{H}}, \quad \rho_0 \alpha_{\beta^{(i,o)}} = \left\langle f_M^o, \psi_{\beta^{(i,o)}} f_0 \right\rangle_{\mathscr{H}}. \tag{43}$$

With n_o and n_e, we will define the total number of odd and even moments respectively; see (98) for an explicit expression for n_o and n_e. Trivially, $n_o \leq n_e$ with equality only for $d = 1$ and M odd in (2) and (22) respectively [31]. The orthogonality and recursion relations of the Hermite polynomials implies

$$\left\langle \psi_{\beta^{(i,o)}} f_0, \psi_{\beta^{(j,e)}} f_0 \right\rangle_{\mathscr{H}} = 0, \quad \left\langle \psi_{\beta^{(i,e)}} f_0, \xi_1 \psi_{\beta^{(j,e)}} f_0 \right\rangle_{\mathscr{H}} = 0, \quad \left\langle \psi_{\beta^{(i,o)}} f_0, \xi_1 \psi_{\beta^{(j,o)}} f_0 \right\rangle_{\mathscr{H}} = 0, \tag{44}$$

using which, the entropy flux across the boundary in (41) can be simplified

$$\begin{aligned} \int_{\partial\Omega_1}\int_{\mathbb{R}^d} \phi^{(1)}(f_M) d\xi ds = \frac{1}{2}\int_{\partial\Omega_1}\int_{\mathbb{R}^d} \xi_1 f_M^2 f_0^{-1} d\xi ds &= \int_{\partial\Omega_1}\int_{\mathbb{R}^d} \xi_1 f_M^o f_M^e f_0^{-1} d\xi ds \\ &= \int_{\partial\Omega_1} (\alpha^o)^T \mathbf{A}^{oe} \alpha^e ds \end{aligned} \tag{45}$$

where $\alpha^o \in \mathbb{R}^{n_o}$ and $\alpha^e \in \mathbb{R}^{n_e}$ are vectors containing all the odd and the even moments of f_M respectively. The matrix $\mathbf{A}^{oe} \in \mathbb{R}^{n_o \times n_e}$ is given as

$$
\begin{aligned}
A_{ij}^{oe} &= \left\langle \psi_{\beta^{(i,o)}} f_0, \xi_1 \psi_{\beta^{(j,e)}} f_0 \right\rangle_{\mathscr{H}}, \quad i \in \{0, \dots n_o - 1\}, \quad j \in \{0, \dots n_e - 1\} \\
&= \rho_0 \sqrt{\theta_0} \left(\sqrt{m_1^{(i,o)} + 1}\, \delta_{m_1^{(i,o)}+1, m_1^{(j,e)}} + \sqrt{m_1^{(i,o)}}\, \delta_{m_1^{(i,o)}-1, m_1^{(j,e)}} \right) \prod_{p=2}^{d} \delta_{m_p^{(i,o)}, m_p^{(j,e)}}
\end{aligned} \tag{46}
$$

With the ordering of the multi-indices $\beta^{(i)}$ given in subsection 8.1, $\mathbf{A}^{oe}$ has the properties [31]

$$
\mathbf{A}^{oe} = \left(\hat{\mathbf{A}}^{(oe)}, \tilde{\mathbf{A}}^{(oe)} \right), \quad det(\hat{\mathbf{A}}^{(oe)}) \neq 0 \quad \Rightarrow \quad rank(\mathbf{A}^{oe}) = n_o \tag{47}
$$

where $\hat{\mathbf{A}}^{oe} \in \mathbb{R}^{n_o \times n_o}$ and $\tilde{\mathbf{A}}^{oe} \in \mathbb{R}^{n_o \times (n_e - n_o)}$ (recall $n_e > n_o$).

The entropy flux in (45) can be further simplified through a suitable set of boundary conditions. Along $\partial\Omega_1$, we know that by prescribing a value to all the odd variables we obtain the correct number of boundary conditions [9, 17, 28, 31, 35]. Thus, the boundary conditions along $\partial\Omega_1$ can be formally given as

$$
\alpha^o = \mathbf{M}\alpha^e + \mathbf{g} \quad \text{in} \quad \partial\Omega_1 \times (0, T] \tag{48}
$$

where $\mathbf{M} \in \mathbb{R}^{n_o \times n_e}$ and the boundary inhomogeneity $\mathbf{g} \in \mathbb{R}^{n_o}$ smoothly depends upon $\tilde{\rho}_{in}$ and $\tilde{\theta}_{in}$. Since the moment system resulting from (21) will be a linear hyperbolic system, we can avoid discontinuities in its solution, and thus obtain a strong solution, by having (i) smooth initial conditions, (ii) initial conditions which are compatible with the boundary conditions and (iii) smooth boundary data $\mathbf{g}$ [6, 29]. The smoothness of the initial conditions and the boundary data $\mathbf{g}$ follow from the assumptions made on the initial data (7) and the boundary conditions (8). The compatibility between the initial and the boundary conditions can be ensured by a careful choice of the initial conditions. Assuming the conditions (i) to (iii) to be satisfied, for the further discussion, we can assume that the moment system will have a strong solution. As a result, the values of the moments at the boundary will be well defined and we can replace the boundary conditions from (48) into the entropy flux across the boundary in (45), to obtain

$$
-\int_{\partial\Omega_1} (\alpha^o)^T \mathbf{A}^{oe} \alpha^e ds = -\int_{\partial\Omega_1} \left[(\alpha^e)^T \mathbf{M}^T \mathbf{A}^{oe} \alpha^e + \mathbf{g}^T \mathbf{A}^{oe} \alpha^e \right] ds \tag{49}
$$

From (49), it clear that in order to satisfy (41) we need certain constraints on $\mathbf{M}$; these conditions will be the necessary and the sufficient conditions for the entropy stability of the approximation in (22).

Theorem 3.1. *Let a quadratic form $\mathscr{M}$ be defined as*

$$
\mathscr{M} = -\left((\alpha^q)^T \mathbf{M}^T \mathbf{A} \alpha^q + \mathbf{g}^T \mathbf{A} \alpha^q \right) \tag{50}
$$

where $\mathbf{A} \in \mathbb{R}^{p \times q}$ $(p < q)$ is a constant matrix, $rank(\mathbf{A}) = p$ and $\mathbf{g} \in \mathbb{R}^p$ is independent of α^q. Let κ be some factor independent of α^q then, $\mathscr{M} \leq \kappa$, for all $\alpha^q \in \mathbb{R}^q$, if and only if

$$
\mathbf{M} = \mathbf{L}\mathbf{A} \quad \textit{and} \quad \mathbf{g} \in range(sym(\mathbf{L})) \tag{51}
$$

where $\mathbf{L}$ is a constant positive semi-definite matrix and $sym(\mathbf{L})$ is the symmetric part of $\mathbf{L}$.

Proof. See subsection 8.2. □

Comparing the entropy flux in (49) and the boundary conditions in (48) with the general framework developed in Theorem 3.1, we find

Corollary 3.1. *Under the assumption that $\tilde{\rho}_{in}$ and $\tilde{\theta}_{in}$ are arbitrarily chosen, which implies that* $\mathbf{g}$ *in* (48) *is arbitrary, the approximation* (22) *can be entropy stable, in the sense of* (39)*, if and only if*

(i) $\mathbf{M} = \mathbf{L}\mathbf{A}^{oe}$.

(ii) $\mathbf{L}$ *is positive definite.*

We will call the boundary conditions in (48) with $\mathbf{M} = \mathbf{L}\mathbf{A}^{oe}$, the *Onsager boundary conditions* (OBCs) with a positive definite $\mathbf{L}$ being the *Onsager matrix* [28, 31]. The invertibility requirement on $\mathbf{L}$ ensures that any arbitrary $\mathbf{g}$ belongs to its range. In order to come up with an explicit expression for the *Onsager matrix* and the boundary inhomogeneity $\mathbf{g}$, we will take the help of the continuity of odd fluxes proposed in [17].

Remark 11. In (45), α^o can be looked upon as the forces with $\mathbf{A}^{oe}\alpha^e$ being their corresponding fluxes [24, 28, 35]. Therefore, the authors in [28, 31, 34], have restricted the *Onsager matrix* to be *s.p.d* so as to obtain equal contribution from the forces (α^o) and the fluxes ($\mathbf{A}^{oe}\alpha^e$) into the entropy flux. But anyhow only the symmetric part of the *Onsager matrix* appears in the entropy flux, see subsection 8.2, and therefore, it is sufficient to consider the *Onsager matrix* to be positive definite.

Remark 12. In [1], the authors look for an entropy stable DG approximation of a particular moment approximation such that the entropy dissipation inequality in (12) is reproduced on a spatially discrete level. But in the present work we focus upon having a solution independent upper bound on the total entropy in the domain, on a spatially continuous level. Entropy stability, on a spatially discrete level, can then be achieved by using an entropy stable numerical scheme, in the physical space, to further discretize the entropy stable moment approximation.

3.3 Continuity of Odd Fluxes

To prescribe the correct number of boundary conditions, we would like to prescribe the odd moments in terms of the even ones through a relation of the type (48). Therefore, to obtain boundary conditions for the moment approximation, we would like to approximate the behaviour of the first n_o odd moments of f at the boundary.

Behaviour of the Kinetic Solution at the Boundary: Grad [17] proposed the idea of continuity of odd fluxes based upon his observations made on a specular wall; see [33] for details. In the present work, we will motivate this idea using the behaviour of the solution to the linearised BE (2) at the boundaries, the continuity of odd fluxes will then follow as an approximation to this behaviour.

In order to obtain the governing relation for all the odd moments of f, we test the kinetic boundary conditions (8) by all the odd basis functions $\psi_{\beta^{(i,o)}}$ to obtain, after certain manipulations [39],

$$\frac{1}{2}\int_{\mathbb{R}^d} \psi_{\beta^{(i,o)}} f^o d\xi = \int_{\mathbb{R}^{d-1}} \int_{\xi_1>0} \psi_{\beta^{(i,o)}} f^e d\xi + \int_{\mathbb{R}^{d-1}} \int_{\xi_1<0} \psi_{\beta^{(i,o)}} f_{in} d\xi, \quad i \in \mathbb{N} \tag{52}$$

where f^o and f^e are the odd and even parts of f with respect to ξ_1. Using the expansion for f from (35) in (52), the relation in (52) can also be expressed in as

$$(\alpha^o)^{(BE)} = \mathbf{M}^{(BE)} (\alpha^e)^{(BE)} + \mathbf{g}^{(BE)} \quad \text{in} \quad \partial\Omega_1 \times (0,T] \tag{53}$$

where $(\alpha^o)^{(BE)}$ and $(\alpha^e)^{(BE)}$ contain all the odd and even moments of f respectively. The operator $\mathbf{M}^{(BE)}$

and the series $\mathbf{g}^{(BE)}$ are given as

$$M_{ij}^{(BE)} = \frac{2}{\rho_0}\int_{\mathbb{R}^{d-1}}\int_{\xi_1>0} \psi_{\beta^{(i,o)}}\psi_{\beta^{(j,e)}} f_0 d\xi \tag{54a}$$

$$g_i^{(BE)} = \frac{2}{\rho_0}\int_{\mathbb{R}^{d-1}}\int_{\xi_1<0} \psi_{\beta^{(i,o)}} f_{in} d\xi \quad \forall \quad i,j \in \mathbb{N}. \tag{54b}$$

We note that the relation in (53) is not an approximation but is rather the exact behaviour of the true odd and even moments of the kinetic solution at the boundary.

An Approximation to the Boundary Behaviour: Due to the discontinuity of the distribution function at the boundary, even the first n_o odd moments in (53) see a contribution from those even moments which have $|\beta^{(i,e)}|> M$. This contribution from the higher order even moments needs to be approximated if we wish to find a boundary relation for the n_o odd moments appearing in f_M. One of the easiest possible ways to achieve this, and the one that has been used in many other works [17, 28, 33, 35], could be to ignore the contribution from all the even moments with $|\beta^{(i,e)}|> M$; the methodology is equivalent to replacing f by f_M in (52) which is well known in the literature as the continuity of odd fluxes [17]. This leads to

$$\alpha^o = \mathbf{M}^{(in)}\alpha^e + \mathbf{g}^{(in)} \quad \text{in} \quad \partial\Omega_1 \times (0,T] \tag{55}$$

where $\alpha^o \in \mathbb{R}^{n_o}$ and $\alpha^e \in \mathbb{R}^{n_e}$. The matrix $\mathbf{M}^{(in)} \in \mathbb{R}^{n_o \times n_e}$ and the vector $\mathbf{g}^{(in)} \in \mathbb{R}^{n_o}$ are the upper left $n_o \times n_e$ matrix block of $\mathbf{M}^{(BE)}$ and the first n_o elements of $\mathbf{g}^{(BE)}$ respectively

$$M_{ij}^{(in)} = M_{ij}^{(BE)} \quad i \in \{0,\dots n_o-1\}, \quad j \in \{0,\dots n_e-1\} \tag{56a}$$

$$g_i^{(in)} = g_i^{(BE)} \quad i \in \{0,\dots n_o-1\}. \tag{56b}$$

The relation in (55) is an approximation to (53) and so we make an error in capturing the kinetic boundary conditions. We will now discuss whether the boundary conditions, given in (55), lead to entropy stability or not.

Entropy Instability: The entropy stability of the approximation (22), with the boundary conditions given in (55), does not immediately follows from the entropy stability of the linearised BE due to the following reason. The entropy flux for the linearised BE along $\partial\Omega_1$ can also be expressed as

$$\begin{aligned} -\frac{1}{2}\int_{\partial\Omega_1}\int_{\mathbb{R}^d} \xi_1 f^2 f_0^{-1} d\xi ds &= -\frac{1}{2}\int_{\partial\Omega_1}\int_{\mathbb{R}^d} \xi_1 \left[(\Pi_M f)^2 + 2\Pi_M f R + R^2\right] f_0^{-1} d\xi ds \\ &\leq H(t) \end{aligned} \tag{57}$$

where Π_M is as defined in (26), $R = f - \Pi_M f$ and the inequality exists because of the entropy stability of the linearised BE. If we replace $R = 0$ in (57), which we have done in order to obtain (55) from (52), then it is not clear whether the inequality will still hold true or not. Hence, by removing the contribution from all the higher order even moments, we might endanger the entropy stability of the linearised BE.

The boundary conditions in (55) have the same form as (48) and therefore, due to Theorem 3.1, they can lead to entropy stability (or a bound of the type (41)) if and only if $\mathbf{M}^{(in)} = \mathbf{L}\mathbf{A}^{oe}$ with $\mathbf{L}$ being positive definite. For any hopes of the matrix $\mathbf{M}^{(in)}$ being of the desired form, the following condition must be satisfied

$$\mathcal{N}(\mathbf{A}^{oe}) \subseteq \mathcal{N}(\mathbf{M}^{(in)}) \tag{58}$$

where $\mathcal{N}(.)$ represents the null-space of a matrix. The satisfaction of (58) will ensure that $\mathbf{M}^{(in)}$ can be

expressed as $\mathbf{M}^{(in)} = \mathbf{L}\mathbf{A}^{oe}$ with $\mathbf{L}$ being some matrix. Then, one can check whether $\mathbf{L}$ is positive definite or not to fully determine the stability of the boundary conditions in (55). In [31, 41], the condition in (58) was derived, using characteristic splitting, as one of the necessary conditions for the entropy stability of the boundary conditions for a gas-wall interaction. Concerning (58), for an arbitrary value of M in (22), we have the result

Lemma 3.1. *Assuming $M \geq 2$ and $d \leq 3$, the boundary conditions, given in (55), obtained from the continuity of odd fluxes satisfy (58) if and only if $d = 1$ in (2) and M is odd in (22).*

Proof. See subsection 8.3. □

The result in Lemma 3.1 shows that the boundary conditions, in (55), lead to entropy instability for a large class of approximations (22). We will now discuss a methodology to stabilize the boundary conditions in (55) such that we obtain entropy stability. For the coming discussion, we will be assuming d and M to be such that the relation in (58) is not satisfied. For $d = 1$ and M odd, the boundary conditions obtained through the continuity of odd fluxes leads to stability; see [31] for details.

3.4 Entropy Stabilization

Every row of the matrix $\mathbf{M}^{(in)}$ can be decomposed into two parts: (i) one part which belongs to the row range of $\mathbf{A}^{oe}$ and (ii) the other part which lies outside of the row range of $\mathbf{A}^{oe}$. Due to Lemma 3.1, the second part is the one which makes $\mathbf{M}^{(in)}$ dissatisfy (58) and will thus be non-zero. Hence, we can decompose $\mathbf{M}^{(in)}$ as

$$\mathbf{M}^{(in)} = \mathbf{R}\mathbf{A}^{oe} + \bar{\mathbf{M}} \tag{59}$$

where $\bar{\mathbf{M}} \in \mathbb{R}^{n_o \times n_e}$, $\mathbf{R}$ is some matrix and $\mathcal{N}(\mathbf{A}^{oe}) \not\subseteq \mathcal{N}(\bar{\mathbf{M}})$. By adding and subtracting $\mathbf{L}\mathbf{A}^{oe}$ from $\mathbf{M}^{(in)}$, $\mathbf{L}$ being a positive definite matrix, we can also express $\mathbf{M}^{(in)}$ as

$$\mathbf{M}^{(in)} = \mathbf{L}\mathbf{A}^{oe} + \tilde{\mathbf{M}} \tag{60}$$

where $\tilde{\mathbf{M}} = (\mathbf{R} - \mathbf{L})\mathbf{A}^{oe} + \bar{\mathbf{M}}$; again $\mathcal{N}(\mathbf{A}^{oe}) \not\subseteq \mathcal{N}(\tilde{\mathbf{M}})$. From the results in Theorem 3.1, we know that the presence of $\tilde{\mathbf{M}}$ in (60) is the reason why the boundary conditions in (55) lead to entropy instability. Therefore, one of the possible ways to obtain entropy stability from (60) is to completely remove the contribution of $\tilde{\mathbf{M}}$ from $\mathbf{M}^{(in)}$ by defining a matrix $\mathbf{M}^{(in,*)}$ as

$$\mathbf{M}^{(in,*)} = \mathbf{M}^{(in)} - \tilde{\mathbf{M}} = \mathbf{L}\mathbf{A}^{oe}. \tag{61}$$

Then by replacing $\mathbf{M}$ by $\mathbf{M}^{(in,*)}$ and $\mathbf{g}$ by $\mathbf{g}^{(in)}$ in (48), we will obtain a set of OBCs which will lead to entropy stability due to Theorem 3.1.

The entropy stabilization of $\mathbf{M}^{(in)}$, with the help of an $\mathbf{M}^{(in,*)}$, can also be understood by recalling the entropy bound for the moment approximation which reads

$$d_t S(f_M) \leq -\int_{\partial\Omega_1} \phi^+ ds - \int_{\partial\Omega_1} \phi^- ds \tag{62}$$

where

$$\phi^+ = \left[(\mathbf{A}^{oe}\alpha^e)^T \mathbf{L}^T \mathbf{A}^{oe}\alpha^e + \mathbf{g}^T \mathbf{A}^{oe}\alpha^e \right], \quad \phi^- = \left[\left(\tilde{\mathbf{M}}\alpha^e\right)^T \mathbf{A}^{oe}\alpha^e \right] \tag{63}$$

In expressing (62), we have used the boundary conditions (55) and the decomposition of the boundary matrix $\mathbf{M}^{(in)}$ from (60). Due to Theorem 3.1, the contributions ϕ^+ and ϕ^- appearing in (62) represent

that part of the entropy flux which leads to a bounded and an unbounded growth of $S(f_M)$. Therefore, entropy stability can be obtained by adding an additional entropy flux $\int_{\partial\Omega_1}\tilde{\phi}ds = -\int_{\partial\Omega_1}\phi^- ds$ across the boundary, through the boundary conditions, which negates the influence of ϕ^- and provides us with a bounded growth for $S(f_M)$

$$d_t S(f_M) \leq -\int_{\partial\Omega_1}\phi^+ ds - \int_{\partial\Omega_1}\phi^- ds - \int_{\partial\Omega_1}\tilde{\phi}ds = -\int_{\partial\Omega_1}\phi^+ ds \leq H(t) \tag{64}$$

thus leading to a bounded growth for $S(f_M)$.

Every different decomposition in (60) leads to a different *Onsager matrix* and hence, the choice of the *Onsager matrix* is not unique. One of the possible methodologies to come up with a model for the *Onsager matrix* could be to construct an $\mathbf{M}^{(in,*)}$ such that it has the same first n_o columns a $\mathbf{M}^{(in)}$ [28, 31, 34]. Using this methodology, and noting that the first n_o columns of $\mathbf{M}^{(in)}$ and $\mathbf{M}^{(in,*)}$ are given by $\hat{\mathbf{M}}^{(in)}$ and $\mathbf{L}^{(in)}\hat{\mathbf{A}}^{(oe)}$ respectively, we can obtain an explicit expression for the *Onsager matrix*

$$\mathbf{L}^{(in)}\hat{\mathbf{A}}^{(oe)} = \hat{\mathbf{M}}^{(in)} \quad \Rightarrow \quad \mathbf{L}^{(in)} = \hat{\mathbf{M}}^{(in)}\left(\hat{\mathbf{A}}^{(oe)}\right)^{-1}. \tag{65}$$

where the invertibility of $\hat{\mathbf{A}}^{(oe)}$ follows from (46). The positive definiteness of $\mathbf{L}^{(in)}$ then follows from the result

Theorem 3.2. *The matrix* $\mathbf{L}^{(in)}$ *given by* (65) *is s.p.d.*

Proof. See subsection 8.4. □

Thus the matrix $\mathbf{M}^{(in,*)}$ with the matrix $\mathbf{L}$ given by $\mathbf{L}^{(in)}$ fulfils all the requirements for entropy stability formulated in Theorem 3.1 for the boundary inhomogeneity $\mathbf{g}^{(in)}$. By replacing the boundary matrix $\mathbf{M}$ by $\mathbf{M}^{(in,*)}$ and $\mathbf{g}$ by $\mathbf{g}^{(in)}$ in (48), we can obtain the boundary conditions, which lead to entropy stability of (22), through the relation

$$\alpha^o = \hat{\mathbf{M}}^{(in)}\left(\hat{\mathbf{A}}^{(oe)}\right)^{-1}\mathbf{A}^{oe}\alpha^e + \mathbf{g}^{(in)} \quad \text{in} \quad \partial\Omega_1 \times (0,T]. \tag{66}$$

In [41], it was shown that the approximation (22) provides a hierarchical framework for approximating the solution to the linearised BE. Corresponding to a particular value of M, for the present discussion, a matrix will be said to have a hierarchical structure if it contains the matrices corresponding to all the lower values of M. Since we are dealing with IBVPs, in addition to $\mathbf{A}^{oe}$, the OBCs in (66) should also have a hierarchical structure (only then we will obtain a hierarchical approximation of the IBVP((2), (8) and (7))). The hierarchical nature of the matrix $\mathbf{M}^{(in)}$ is clear from its definition itself (56a) but it leads to entropy instability (see Lemma 3.1) and therefore cannot be used for realistic simulations. We will now show, with the help of examples, that the OBCs given in (66) preserve the hierarchical nature of the matrix $\mathbf{M}^{(in)}$.

The OBCs (66) consist of three parts (i) the matrix $\mathbf{A}^{oe}$, (ii) The *Onsager matrix* $\mathbf{L}^{(in)}$ given by (65) and (iii) the inhomogeneity $\mathbf{g}^{(in)}$ given by (56b). The hierarchical structure of the matrix $\mathbf{A}^{oe}$ (46) and the inhomogeneity $\mathbf{g}^{(in)}$ (56b) is clear from their definitions itself. To demonstrate the hierarchical nature of $\mathbf{L}^{(in)}$ we can consider its matrix plot, corresponding to $M = 7$ ($d = 3$), shown in Figure 1. From Figure 1 it is clear that the *Onsager matrix* for $M = 7$ contains the *Onsager matrices* corresponding to all the lower values of M thus demonstrating the hierarchical structure of the OBCs; a computational analysis shows that the hierarchy of the *Onsager matrices* is maintained atleast up till $M = 20$ and supports the claim that the OBCs are a hierarchical approximation to the boundary conditions of the linearised BE.

Extension to Curved Domains : A detailed extension of the presented framework to curved domains is beyond the scope of the present work. Therefore, we will briefly summarise the methodology which

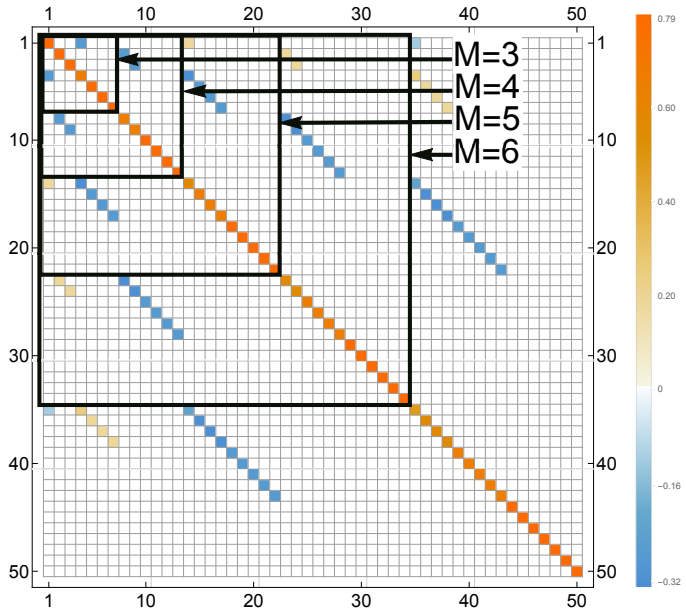

Figure 1: Matrix plot of the *Onsager matrix* corresponding to $M = 7$. The plot demonstrates the hierarchical nature of the *Onsager matrices* which results into a hierarchical structure of the OBCs.

can be used to extend the framework presented to curved domains. The entropy flux across the boundary $\partial\Omega$ of some bounded domain Ω can be expressed as

$$\int_{\partial\Omega}\int_{\mathbb{R}^d} \phi^{(i)}(f_M) n_i d\xi ds = \frac{1}{2}\int_{\partial\Omega}\int_{\mathbb{R}^d} \xi_n f_M^2 f_0^{-1} d\xi ds = \int_{\partial\Omega} \alpha^T \mathbf{A}^{(n)} \alpha ds \tag{67}$$

where $\mathbf{n}$ represent a unit normal perpendicular to $\partial\Omega$ and points out of the domain, the flux matrix $A_{ij}^{(n)} = \left\langle \psi_{\beta^{(i)}} f_0, \xi_n \psi_{\beta^{(j)}} f_0 \right\rangle_{\mathscr{H}}$ and α contains all the coefficients $\alpha_{\beta^{(i)}}$. Due to the rotational invariance of the moment systems based upon tensorial Hermite polynomials, it can be shown that there exists an orthogonal matrix $\mathbf{P}$ such that [13, 24, 41]

$$\mathbf{A}^{(n)} = \mathbf{P}^T \mathbf{A}^{(1)} \mathbf{P}, \quad \mathbf{A}^{(1)} = \begin{pmatrix} 0 & \mathbf{A}^{oe} \\ (\mathbf{A}^{oe})^T & 0 \end{pmatrix}. \tag{68}$$

Using (68) in (67), we can simply the entropy flux to

$$\int_{\partial\Omega}\int_{\mathbb{R}^d} \phi^{(i)}(f_M) n_i d\xi ds = \int_{\partial\Omega} (\alpha_n^o)^T \mathbf{A}^{oe} \alpha_n^e ds, \quad \begin{pmatrix} \alpha_n^o \\ \alpha_n^e \end{pmatrix} = \mathbf{P} \begin{pmatrix} \alpha^o \\ \alpha^e \end{pmatrix} \tag{69}$$

where $\alpha_n^o \in \mathbb{R}^{n_o}$ and $\alpha_n^e \in \mathbb{R}^{n_e}$ can be looked upon as the odd and even moments of f with respect to the normal direction $\mathbf{n}$. Comparing the entropy flux in (69) with the general form presented in Theorem 3.1 we can conclude that a set of boundary conditions given by

$$\alpha_n^o = \mathbf{L}^{(in)} \mathbf{A}^{oe} \alpha_n^e + \mathbf{g}_n^{(in)}$$

will lead to entropy stability.

Remark 13. The integrals appearing in $\hat{\mathbf{M}}^{(in)}$ (56a) are only half space along the ξ_1 direction. Therefore, for the other two directions (ξ_2 and ξ_3), we can use the orthogonality of the Hermite polynomials (16a) which results in $\hat{\mathbf{M}}^{(in)}$ begin a sparse matrix. The sparsity of $\hat{\mathbf{A}}^{(oe)}$ (47) is clear from the orthogonality of the even and odd basis functions (44). The sparsity of $\mathbf{M}^{(in)}$ and $\hat{\mathbf{A}}^{(oe)}$ is the reason for the sparsity of the *Onsager matrix* appearing in Figure 1.

Remark 14. By keeping the first n_o columns in $\mathbf{M}^{(in,*)}$ to be the same as $\hat{\mathbf{M}}^{(in)}$, we ensure that the entropy stabilizing boundary flux ($\int_{\partial\Omega}\tilde{\phi}ds$) appearing in (64) will only depends upon the highest order even moments ($\tilde{\mathbf{M}}^{(in)}$ will only have a contribution in the last $n_e - n_o$ rows). If one further assumes that the magnitude of the the highest order even moment reduces as the value of $M \to \infty$ then it might be possible to show that $\tilde{\phi} \to 0$, in some suitable norm, as $M \to \infty$ which can further help us in rigorously showing the convergence of f_M to f. Therefore, the methodology of keeping the coefficients of the first n_o moments to be the same, while constructing $\mathbf{M}^{(in,*)}$, might not just be a modelling assumption but might also be closely related to the convergence of our moment approximation.

4 Prescribing the Inflow Velocity

For many practical applications, it is required to prescribe the normal component of the velocity along the inflow boundary $\partial\Omega^+$ i.e. it is required to prescribe some $\hat{v}_n = \tilde{v}_i n_i$ (n_i is a unit normal pointing out of the domain). We will now discuss the entropy bounds of two methods, for both the linearised BE and its moment approximation, which could be used to achieve the desired $\hat{v}_n$ and will show that one of these methods always leads to entropy instability.

4.1 The linearised Boltzmann Equation

The prescription of $\hat{v}_n$ along $\partial\Omega$ can be summarised through the relation

$$\tilde{v}_i n_i = \int_{\mathbb{R}^d} \xi_n f d\xi = \int_{\mathbb{R}^{d-1}}\int_{\xi_n>0} \xi_n f d\xi + \int_{\mathbb{R}^{d-1}}\int_{\xi_n<0} \xi_n f_{in} d\xi = \hat{v}_n, \quad \text{in} \quad \partial\Omega^+ \times (0,T] \tag{70a}$$

$$f_{in} = f_{\mathscr{M}}(\xi; \tilde{\rho}^{(\pm)}, 0, \tilde{\theta}^{(\pm)}), \quad \text{in} \quad \partial\Omega^{\pm} \times (0,T]. \tag{70b}$$

where $\mathbf{n}$ is a unit normal perpendicular to the boundary and points out of the domain. Clearly, in order to compute $\hat{v}_n$, we require the value of the distribution function, along the whole boundary $\partial\Omega^+$, for all the velocities $\xi \in \mathbb{R}^d$. But at the boundary, prior to any computation, we only know the distribution function corresponding to those velocities which have $\xi_n < 0$ (i.e. we only know f_{in}). This leaves us with two possible methodologies to prescribe $\hat{v}_n$

Method1 Assuming $\tilde{\rho}^+$ to be a free parameter, we can compute it from (70a) by using (70b)

$$\begin{aligned}\frac{\tilde{\rho}^+}{\rho_0} = &\frac{1}{\int_{\mathbb{R}^{d-1}}\int_{\xi_n>0}\xi_n f_0(\xi)d\xi}\left[\int_{\mathbb{R}^{d-1}}\int_{\xi_n>0}\xi_n f(\mathbf{x},\xi,t)d\xi\right.\\ &\left.-\frac{\tilde{\theta}^+}{2\theta_0}\int_{\mathbb{R}^{d-1}}\int_{\xi_n>0}\xi_n\left(\frac{\xi_i\xi_i}{\theta_0}-3\right)f_0 d\xi - \hat{v}_n(\mathbf{x},t)\right].\end{aligned} \tag{71}$$

Substituting $\tilde{\rho}^+$ into f_{in} given in (70b), provides us with fully defined boundary conditions which ensure a particular normal velocity $\hat{v}_n$ along $\partial\Omega^+$. Note that for $\hat{v}_n = 0$, we recover the expression for $\tilde{\rho}^+$ corresponding to a stationary wall [30, 33].

Method2 We can prescribe some initial $\tilde{\rho}^{(\pm)}$ and then compute the normal flow velocity generated along $\partial\Omega^+$. By comparing the desired normal velocity, $\hat{v}_n$, with the one obtained, we can change $\tilde{\rho}^{(\pm)}$ with the help of a feedback loop and continue iterating until the desired inflow velocity is reached. Recently in [4], such a methodology was used to prescribe a particular heat flux at the gas-wall interface using DSMC.

For the simplicity of the analysis which follows, we will assume $\tilde{\theta}_{in} = 0$ along the whole boundary. Comparatively, *Method1* is less computationally expensive than *Method2* due to the absence of any iteration step. But, only that method which leads to entropy stability can be used for realistic computations.

In *Method2*, at any given iteration step, both the quantities $\tilde{\rho}^{(\pm)}$ are the given data of the problem and are independent of the solution. Therefore, we can directly use the bound in (33), which would lead us to the same entropy estimate as that given in (34); this proves the entropy stability of *Method2*. On the other hand, the entropy estimate for *Method1* is given by the result

Lemma 4.1. *Using Method1, we obtain the entropy estimate*

$$d_t S(f) \leq H(t) - \frac{2}{\beta}\left(\oint_{\partial\Omega} \hat{v}_n \left[\int_{\mathbb{R}^{d-1}} \int_{\xi_n>0} \xi_n f_e d\xi\right] ds\right) \tag{72}$$

where f_e is the even part of f with respect to ξ_n and $\beta = \int_{\mathbb{R}^{d-1}} \int_{\xi_n>0} \xi_n f_0(\xi) d\xi$.

Proof. See subsection 8.5 □

Corollary 4.1. *For Method1, the bound for the entropy functional is not solely dependent upon the given data of the problem but is rather also dependent upon the solution through the integral on the boundary. This shows the entropy instability of Method1 and therefore it is preferable to use Method2 for prescribing an inflow velocity.*

Remark 15. It is well understood that the physical state of the gas along $\partial\Omega^+$ is also influenced by the boundary conditions along $\partial\Omega^-$ through the distribution function corresponding to $\xi_n \geq 0$. But *Method1* ignores this fact and rather tries to change the inflow velocity by just using the information along $\partial\Omega^+$; therefore, the entropy instability of *Method1* is no surprise. We will now show that a similar entropy instability exists for the moment approximation (21) while using *Method1*.

4.2 The Moment Approximation

For the sake of discussion, we will consider the boundary face at $\partial\Omega_1$ (face of our cubic domain at $x = 1$) to be a union of two non-overlapping surfaces, $\partial\Omega_1^+$ and $\partial\Omega_1^-$, which correspond to the inflow and the outflow boundary respectively. To maintain a particular inflow velocity along $\partial\Omega_1^+$ we require

$$\tilde{v}_1 = \hat{v}_1 \quad \text{or} \quad \int_{\mathbb{R}^d} \xi_1 f_M d\xi = \int_{\mathbb{R}^d} \xi_1 f_M^o d\xi = \hat{v}_1 \quad \text{in} \quad \partial\Omega_1^+ \times (0,T] \tag{73}$$

where we have used $\int_{\mathbb{R}^d} \xi_1 f_M^e d\xi = 0$, $\hat{v}_1$ is the desired inflow velocity and $\tilde{v}_1$ is the deviation of velocity from the ground state upto $\mathscr{O}(\varepsilon)$. Similar to the analysis for the linearised BE, we will assume f_{in} to be given by (70b). Then, assuming $\tilde{\theta}_{in} = 0$ along the boundary, $\tilde{\rho}^+$ appearing in f_{in} can be computed such that (73) is satisfied which provides us with

$$\frac{\tilde{\rho}^+}{\rho_0} = \frac{1}{\beta}\left[\int_{\mathbb{R}^{d-1}} \int_{\xi_1>0} \xi_1 f_M^e d\xi - \frac{1}{2}\hat{v}_1\right], \quad \left(\beta = \int_{\mathbb{R}^{d-1}} \int_{\xi_1>0} \xi_1 f_0(\xi) d\xi\right) \tag{74}$$

and is the same as (71) but with f replaced by f_M. Along $\partial\Omega_1^+$, similar to (48), we would like to prescribe a boundary relation for all the odd variables (α^o). For entropy stability, due to Theorem 3.1, the boundary relation should be of the form

$$\alpha^o = \mathbf{L}^+ \mathbf{A}^{oe} \alpha^e + \mathbf{g}^+ \quad \text{in} \quad \partial\Omega_1^+ \times (0,T]. \tag{75}$$

where $\mathbf{L}^+$ is some positive definite matrix and $\mathbf{g}^+$ is a solution independent inhomogeneity which we require to be in the range of $sym(\mathbf{L}^+)$; for the present case $\mathbf{g}^+$ will solely depend upon $\hat{v}_1$ ($\tilde{\theta}_{in} = 0$). The explicit expressions for $\mathbf{L}^+$ and $\mathbf{g}^+$ are not of much importance to us, rather by just studying the structure of $\mathbf{L}^+$ and $\mathbf{g}^+$ we will be able to conclude that the conditions for entropy stability are not satisfied. The first variable in α^o corresponds to $\tilde{v}_1$ and therefore the first boundary relation in (75) reads $\tilde{v}_1 = \mathbf{l}_1^T \mathbf{A}^{oe} \alpha^e + g_0^+$, where g_0^+ is the first component of the vector $\mathbf{g}^+$ and $\mathbf{l}_1^T$ is the first row of $\mathbf{L}^+$. Since we require $\tilde{v}_1 = \hat{v}_1$, where $\hat{v}_1$ is independent of the solution, this implies $g_0^+ = \hat{v}_1$ and for all $\alpha^e \in \mathbb{R}^{n_e}$

$$\mathbf{l}_1^T \mathbf{A}^{oe} \alpha^e = 0 \quad \Rightarrow \quad \mathbf{l}_1^T = 0 \quad (\because rank(\mathbf{A}^{oe}) = n_o) \tag{76}$$

Moreover, the deviation in density ($\tilde{\rho}^+$) is given in terms of the other variables (74) and therefore it does not appear in any of the boundary relations in (75) which implies that the first column of $\mathbf{L}^+$ will also be zero (first entry in α^e is deviation in density). Hence, $\mathbf{L}^+$ will have the structure

$$\mathbf{L}^+ = \begin{pmatrix} 0 & \mathbf{0} \\ \mathbf{0} & \bar{\mathbf{L}} \end{pmatrix} \tag{77}$$

with $\bar{\mathbf{L}} \in \mathbb{R}^{(n_o-1)\times(n_o-1)}$ being a *s.p.d* matrix [31]. As per Theorem 3.1, a necessary condition for the entropy flux along $\partial\Omega_1^+$ to be bounded is to have $\mathbf{g}^+ \in range(sym(\mathbf{L}^+))$. Since the first row and column of $\mathbf{L}^+$ is zero, $\mathbf{g}^+ \notin range(sym(\mathbf{L}^+))$ for any $\hat{v}_1 \neq 0$. Hence, similar to the linearised BE, *Method1* leads to entropy instability for the moment approximation.

For *Method2*, since $\tilde{\rho}^{(\pm)}$ is independent of the solution, by prescribing a set of OBCs (66) along both the inflow and the outflow boundary leads to entropy stability. Therefore, similar to the linearised BE, *Method2* should be used to prescribe a particular inflow velocity.

Remark 16. Choosing $\hat{v}_1 = 0$ in (74) we obtain the same relation for $\tilde{\rho}^+$ as for the stationary gas-wall interface. Since $\hat{v}_1$ does not appear in the explicit expression for $\mathbf{L}^+$ this implies that the explicit expression for $\mathbf{L}^+$ will remain the same as for the stationary gas-wall interface and can be found in [31]; for the same reason $\bar{\mathbf{L}}$ in (77) is *s.p.d*.

Entropy Stabilisation of Method-1 : Though *Method1* is apparently cheaper and easier to implement, as compared to *Method2*, but it leads to entropy instability. This motivates us to modify *Method1*, for the moment approximation, such that the inflow velocity remains as close to the desired inflow velocity profile as possible while maintaining entropy stability. The reason why *Method1* is not entropy stable is because the inhomogeneity $\mathbf{g}^+ \notin range(sym(\mathbf{L}^+))$ which is a result of a zero first row and column appearing in the *Onsager matrix* (77). Therefore, we can stabilize *Method1* by modifying $\mathbf{L}^+$ such that

$$\mathbf{L}_{reg}^+ = \begin{pmatrix} \kappa & \mathbf{0} \\ \mathbf{0} & \bar{\mathbf{L}} \end{pmatrix} \tag{78}$$

where $\kappa \in \mathbb{R}^+/\{0\}$ is some regularisation parameter. Since $\bar{\mathbf{L}}$ is a *s.p.d* matrix, any positive value of κ preserves the positive definiteness of $\mathbf{L}_{reg}^+$, and ensures $\mathbf{g}^+ \in range(sym(\mathbf{L}_{reg}^+))$, which then leads to entropy stability. Replacing an *Onsager matrix* given by (78) into (75), and extracting the first boundary condition, out of the resulting boundary conditions, we find

$$\tilde{v}_1 = \hat{v}_1 + \frac{\kappa}{\rho_0} \sum_{i=0}^{n_e-1} a_i^{oe} \alpha_i^e \tag{79}$$

where $\mathbf{a}^{oe}$ is the first row of $\mathbf{A}^{oe}$. Thus by introducing a regularisation parameter, we do not exactly prescribe the desired inflow velocity and it becomes important to understand how the obtained inflow velocity profile deviates from the desired one, as the value of κ is changed; later, we will conduct an empirical study to understand this.

Due to (79), we can expect to obtain an inflow velocity profile, which will be very close to $\hat{v}_1$, by choosing κ arbitrarily small. But before choosing κ arbitrarily small, we need to understand how the upper bound for entropy depends upon κ. Since $\kappa \to 0$ leads to entropy instability, we can expect the upper bound to be $\mathscr{O}(\kappa^{\gamma})$ with $\gamma < 0$. The precise value of γ, which is equal to one, follows from Lemma 4.2 and shows that an arbitrarily small κ can lead to a significantly high value for the upper bound of entropy. We suspect that such a high value for the bound on entropy can lead to sub-optimal convergence rates for our moment approximation. Hence, we can expect a trade-off, while selecting a value for κ, between a desirable value for our entropy upper bound ($\mathscr{T}(t,\kappa)$ in (80)) and the error obtained for the inflow velocity profile (79).

Lemma 4.2. *Assume the deviation in density and temperature to be given quantities along the outflow boundary $\partial\Omega_1^-$. Then, by prescribing the boundary conditions in (75), with $\mathbf{L}^+$ being replaced by $\mathbf{L}^+_{reg}$, along $\partial\Omega_1^+$ and the boundary conditions of the type (66) along the outflow boundary $\partial\Omega_1^-$ we obtain*

$$d_t S(f_M) \leq \mathscr{T}(t,\kappa) \tag{80}$$

where $\mathscr{T}(t,\kappa)$ is $\mathscr{O}(\kappa^{-1})$.

Proof. See subsection 8.6. □

5 Numerical Results

For the discretization in the physical space, we use a DG scheme based upon a upwind numerical flux and $\mathbb{P}^1$ elements; see [41] for details of our DG scheme. The boundary conditions, in the DG discretization, have been implemented weakly with a penalty matrix based upon characteristic splitting [25]. Due to the linearity of our moment approximation (21), the entropy stability, in the semi-discrete form, of our DG implementation follows from the work done in [14, 25]. We will presently not rigorously discuss the entropy stability of our DG scheme but will rather use it as a tool to understand the physical accuracy of our proposed entropy stable Hermite approximation. The iteration into the steady state has been done with an explicit second order Runge-Kutta scheme, the time step for which has been chosen small enough so as to ensure entropy dissipation [38]. Our complete numerical framework has been implemented in the dealii finite element library [5].

For further discussion, we will consider all the quantities to be non-dimensionalised with the appropriate powers of ρ_0 and θ_0 [33]; for simplicity, we will not use a new notation for the non-dimensionalised variables. Such a non-dimensionalization leads to an introduction of a dimensionless factor, the Knudsen number (Kn), which scales the right hand side of the moment approximation in (21) and is given by [33]

$$\mathrm{K}n = \frac{\tau\sqrt{\theta_0}}{L} \tag{81}$$

where τ is the inverse of the collision frequency and L is some suitably chosen length scale. We will choose $Kn = 0.1$ for all the test cases.

5.1 One Dimensional Flow Problem

In the present problem, we will restrict ourselves to a one dimensional physical, $x \in (-0.5, 0.5)$, and velocity space , $\xi \in \mathbb{R}$ ($d = 1$ in (2)). For the ease of obtaining a kinetic solution, with the help of a sufficiently refined first order discrete velocity scheme [23], we will replace the linearised Boltzmann

collision operator, given in (4), by the linearised BGK collision operator given by [39]

$$Q_{BGK}(f) = -\frac{1}{\mathrm{Kn}}(f - f_{\mathscr{M}}) \tag{82}$$

where $f_{\mathscr{M}}$ is as defined in (5). Note that the linearised BGK collision operator also satisfies (10) with the same η as given by (24) and hence the only contribution into the entropy growth in (23) will be coming from the entropy flux across the boundary. Therefore, we can use all the framework presented in the previous sections for approximating the linearised BGK equation in an entropy stable way. For the DG discretization of the physical space, we have chosen $N = 1000$ elements along the spatial domain.

Boundary Data : For a one dimensional kinetic equation, the incoming distribution function along the boundaries (8) has the form (non-dimensionalised)

$$f_{in}(x,\xi,t) = \frac{1}{(2\pi)^{1/2}}\left(He_0(\xi)\tilde{\rho}_{in}(x,t) + \frac{He_2(\xi)}{\sqrt{2}}\tilde{\theta}_{in}(x,t)\right)\exp\left(-\xi^2/2\right) \tag{83}$$

The parameters appearing in (83) have been given in Table 1. The coefficients mentioned in Table 1 lead

Boundary Conditions		
Boundary location	$\tilde{\rho}_{in}$	$\tilde{\theta}_{in}$
Left Boundary($x = -0.5$)	2.0	1.0
Right Boundary($x = 0.5$)	1.0	1.0

Table 1: Boundary conditions for a pressure driven flow corresponding to a one-dimensional problem.

to a difference of one in the deviation of pressure between the incoming distribution functions at the left ($x = -0.5$) and the right boundary ($x = 0.5$) therefore, we can expect a net pressure driven flow from the left to the right boundary (recall, in the non-dimensionalised setting, the deviation of pressure upto $\mathscr{O}(\varepsilon)$ is given by $\tilde{\rho} + \tilde{\theta}$). Since at both the boundaries, the deviation in densities $\tilde{\rho}_{in}$ is a given quantity, we will be using the OBCs presented in (66) (which then leads to entropy stability).

Physical Accuracy and Convergence : With the help of the present test case, we would like to know how well the sequence of solutions, obtained by increasing the value of M in (25) and using the OBCs (66), approximates the kinetic solution. Note that for the one dimensional flow problem and M odd in (25), the boundary conditions obtained through the continuity of odd fluxes leads to entropy stability and hence, to study the approximation quality of the OBCs, we will only consider even values of M.

To study the convergence behaviour, as the value of M is increased, we will monitor e^{η} given by

$$e^{\eta} = \int_{-0.5}^{0.5}\int_{\mathbb{R}} \eta(f_M - \Pi_M f^{ref})\,d\xi\,dx = \frac{1}{2}\sum_{|\beta^{(i)}|\leq M}\int_{-0.5}^{0.5}\left|\alpha_{\beta^{(i)}} - \alpha^{ref}_{\beta^{(i)}}\right|^2 dx \tag{84}$$

In (84), $\eta(f)$ is as given in (24), f^{ref} is the reference solution and $\alpha^{ref}_{\beta^{(i)}}$ represent the moments of the reference solution. The reason for choosing e^{η} lies in its dependence upon all the moments. Hence, if $e^{\eta} \to 0$ as the value of $M \to \infty$ then we can be assured that the L^2 error in all the moments also goes to zero as the value of M is increased. Fig-2(a) shows the variation of e^{η} with M. Clearly, for the present test case, the approximation (25) with the OBCs presented in (66) seems to converge to the desired kinetic solution, with a convergence order close to one; convergence implicitly implies that OBCs are capable of providing physically accurate solutions. We leave a rigorous convergence analysis as a part of our future work.

In contrast to the oscillatory convergence, with respect to the number of moments, reported in [39], our convergence study depicts monotonic convergence; this can be explained as follows. For the one dimensional kinetic equation, the moment system resulting from (25) can also be looked upon as a discrete velocity scheme with the grid points in the velocity space being the $M+1$ Gauss-Hermite quadrature points [30]. Since the Gauss-Hermite quadrature points are symmetric about the origin, for all even values of M there exists atleast one quadrature point which lies at $\xi = 0$ whereas for odd values of M, none of the quadrature points coincide with $\xi = 0$. As a result, we can expect the approximations with an even value of M to be less accurate as compared to approximations with an odd value of M (kinetic boundary conditions (8) are discontinuous along $\xi = 0$). This leads to an oscillatory convergence behaviour, as the value of M is increased, which is then similar to the result presented in [39]. Therefore, the claim of simply increasing the value of M for greater physical accuracy is not usually correct for boundary value problems. Presently, since we are only considering even values of M, increasing the value of M monotonically improves the physical accuracy in the complete domain.

Fig-2(b) shows the variation of deviation in temperature (upto $\mathscr{O}(\varepsilon)$) obtained through two different Hermite approximations, $M = 6$ and $M = 32$. Towards the interior of the domain, both the approximations provide us with acceptable physical accuracy but near the boundary, a higher value of M is needed to capture the boundary layer correctly.

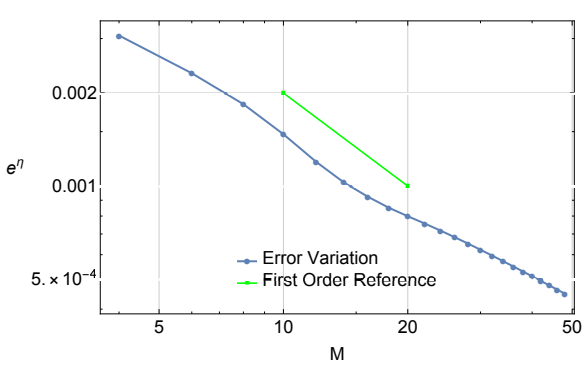

(a) Variation of e^{η} with M for $Kn = 0.1$

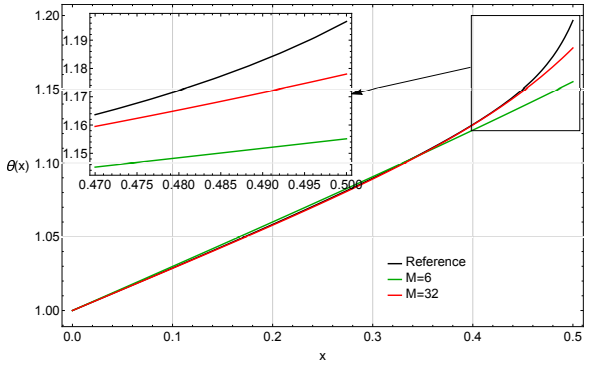

(b) Variation of $\tilde{\theta}$ along x-axis for $M = 6$ and $M = 32$

Figure 2: (a) shows the variation of e^{η} as we increase the value of M being considered. The error has been computed using only even values of M. (b) shows the variation of $\tilde{\theta}$, which is anti-symmetric about the origin, along the domain for $M = 6$ and $M = 32$.

Remark 17. For the reference solution, we have chosen 200 Gauss-Legendre grid points in the velocity space. As has been mentioned earlier, the moment approximation corresponds to a discrete velocity scheme with $M+1$ grid points in the velocity space. Given the low number of grid points in the velocity space for our moment approximation, as compared to the reference solution, the error values in fig-2(a) are acceptable.

5.2 Channel Flow

In order to study the influence of the regularisation parameter κ (79) upon the inflow velocity $\tilde{v}_1$, we conduct an empirical study on a two dimensional rectangular domain in the physical space $\Omega = (-2,2) \times (-0.5,0.5)$ and a three dimensional $\mathbb{R}^3$ velocity space. The collision kernel appearing in (4) will be assumed to correspond to the Maxwell molecules thus, the right hand side in the variational formulation (21) trivially follows from the framework presented in [24, 33, 40]. For the DG discretization, in the physical space, we will use a structured Cartesian mesh with $(N_x, N_y) = 200 \times 200$ elements.

Since, for the present test case, we are not interested in the convergence analysis of our velocity space approximation (25), we will consider $M = 3$ in (25) which corresponds to the Grad's-20 moment system [8].

Boundary Data : We will assume the boundary faces along $y = \pm 0.5$ to be specularly reflecting walls, the boundary conditions for which require all the odd moments, with respect to the y direction (the wall normal), to be zero [17]. Moreover, as is also clear from the structure of the entropy flux (45), specularly reflecting walls do not have any entropy flux associated with them [32]. For the face along $x = 2.0$, we will assume the incoming distribution function to be given by (8) with the parameters as given in Table 2. Along $x = -2.0$, the incoming distribution function will still be given by (8) but with a $\tilde{\rho}_{in}$ now computed through (74) with a $\hat{v}_1$ and $\tilde{\theta}_{in}$ as given in Table 2. Therefore, along $x = 2.0$ we will prescribe boundary conditions given by (66), with a $\mathbf{L}$ as given by (65), whereas along $x = -2.0$ we will prescribe the boundary conditions given by (75) with a $\mathbf{L}^+$ as given by (78). We will chose κ to be the different values in $\{0.001, 0.01, 0.1, 1.0, 2.0\}$.

Boundary Conditions			
Boundary location	$\tilde{\rho}_{in}$	$\tilde{\theta}_{in}$	$\hat{v}_1$
Left Boundary($x = -2.0$)	-	2.0	1.0
Right Boundary($x = 2.0$)	1.0	1.0	-

Table 2: Boundary conditions for the channel flow.

Velocity Profile : Fig-3(d) shows the variation of $\tilde{v}_1$ along the domain for $\kappa = 0.01$. Due to a sufficiently long channel, the flow becomes fully developed after some point along the x-axis. From the study conducted in [39], for fully developed channel flows with specular wall boundaries and no external force, the velocity profile does not vary in the any of the spatial directions and only has an x-component, the constant value of this x-component is such that mass is conserved; this can also be observed from fig-3(d) where the flow appears to be fully developed for $x > 0.0$. Qualitatively, a similar velocity profile, along the domain, was obtained for other values of κ as well. Till some length away from the inflow boundary, $x = -2.0$, we can observe certain boundary effects which are a result of our regularisation (79) and can possibly be explained in the following way. Using (46), the dot product $a_i^{oe}\alpha_i^e$ appearing in (79) can be given as

$$a_i^{oe}\alpha_i^e = \int_{\mathbb{R}^d} \xi_1^2 f_M^e d\xi = \int_{\mathbb{R}^d} \xi_1^2 f_M d\xi \quad \left(\because \int_{\mathbb{R}^d} \xi_1^2 f_M^o d\xi = 0 \right) \tag{85}$$

which is nothing but the flux of momentum (or velocity in the linearised setting) in the x-direction which includes the xx-component of the stress tensor [33]. Therefore, by prescribing an inflow velocity through (79), we might end up introducing a non-zero xx-component of stress at the boundary which then might lead to the development of these boundary effects.

For all the values of κ, as we move away from the wall, the boundary effects which appear close to $x = -2.0$ vanish and the flow becomes fully developed; see fig-3(a) to 3(c). But as we increase the value of κ, as expected, the inflow velocity profile deviates significantly from $\hat{v}_1$. This can be observed through the variation of error in velocity (e^v) and the mass flux (e^m) shown in fig-4 where

$$e^v = \int_{-0.5}^{0.5} |\tilde{v}_1 - 1| dy, \quad e^m = \left| \int_{-0.5}^{0.5} (\tilde{v}_1 - 1) dy \right| \tag{86}$$

Moreover, only for $\kappa \leq 0.1$, it was possible to maintain a positive velocity along $x = -2.0$ and thus a net flow from $x = 2.0$ to $x = -2.0$. For all $\kappa > 0.1$, the term $\kappa a_i^{oe}\alpha_i^e$ (79) dominates the velocity

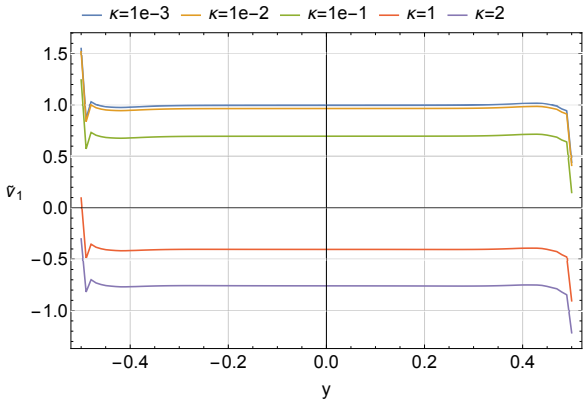

(a) Variation of x-component of velocity ($\tilde{v}_1$) in the y-direction at $x = -2.0$

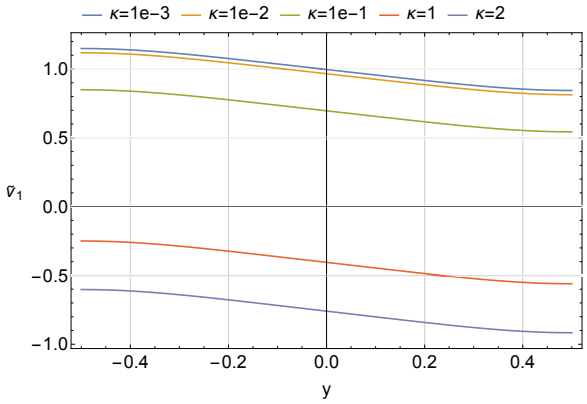

(b) Variation of x-component of velocity ($\tilde{v}_1$) in the y-direction at $x = -1.5$

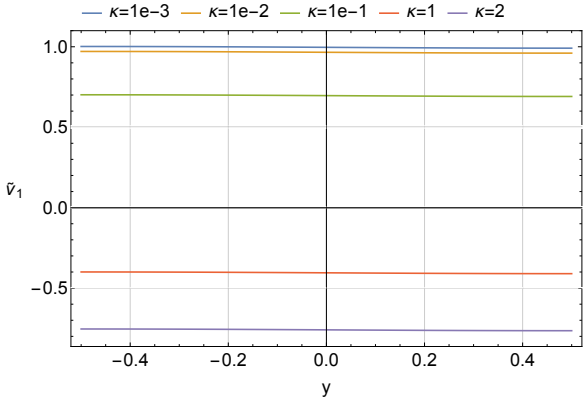

(c) Variation of x-component of velocity ($\tilde{v}_1$) in the y-direction at $x = 0.0$

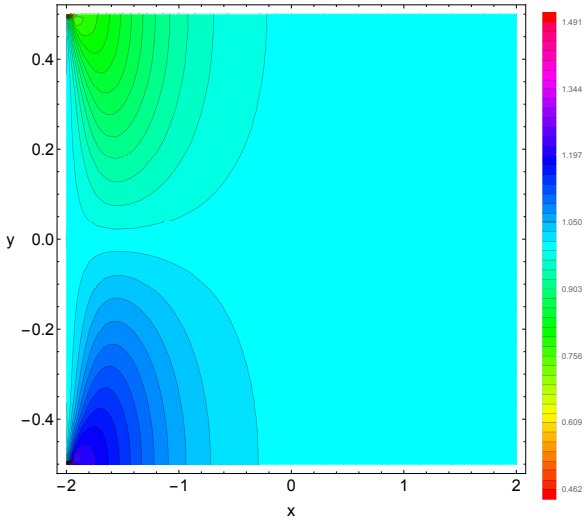

(d) Variation of velocity in the x-direction ($\tilde{v}_1$) along the domain for $\kappa = 0.01$

Figure 3: (a),(b) and (c) show the variation of $\tilde{v}_1$ at different x-locations and for different values of κ. (d) shows the variation of $\tilde{v}_1$ along the whole domain for $\kappa = 0.01$

along $x = -2.0$. And since we do not have any control over the value of $a_i^{oe}\alpha_i^e$, due to the generation of significantly large negative value of $a_i^{oe}\alpha_i^e$, we end up generating a flow in the opposite direction.

Our empirical study shows that by taking a very large value of κ, we not only distort the inflow velocity profile significantly but also end up inducing the wrong flow direction which is undesirable. Therefore, κ cannot be increased beyond a particular value in a hope to obtain a stronger bound on entropy through (80). Neither should one reduce κ beyond a certain point since it might lead to a very large bound for the entropy. Hence, for a given test case, there appears to be a suitable bounded set of positive real numbers from which κ can be chosen from. For the present case, this set appears to be $(0.01, 0.1)$ which might change with the type of test case being used.

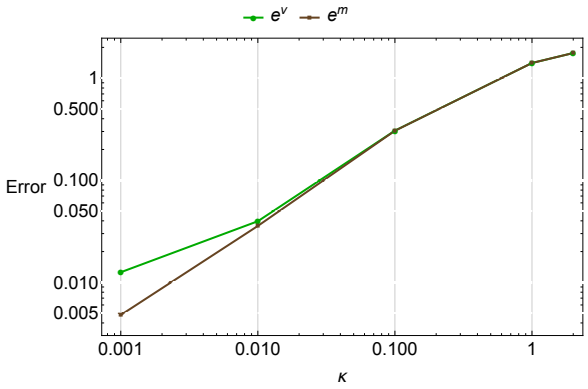

Figure 4: Shows the variation of error in the inflow velocity profile and the mass flux rate for different values of κ.

5.3 Channel Flow Over a Cylinder

With the present test case, we would like to understand whether the proposed entropy stable Hermite approximation can recover certain basic benchmark features of rarefied gas flow for complex geometries. We will consider the physical domain to be given by

$$\Omega = (-2,2)\times(-0.5,0.5)/\left\{(x,y)\in\mathbb{R}^2 | x^2+y^2 < \frac{1}{16}\right\}. \tag{87}$$

which a rectangular domain with a circular hole in the middle and the velocity space will be considered to be $\mathbb{R}^3$. Similar to the previous test case, the collision kernel appearing in (4) will be assumed to correspond to the Maxwell molecules. Mesh, in the physical space, has been created with the help of Gmsh [15] and contains in total 3894 elements with additional refinement near the cylindrical surface fig-5. To maintain sufficient accuracy we use second order isoparametric elements at the cylindrical boundary.

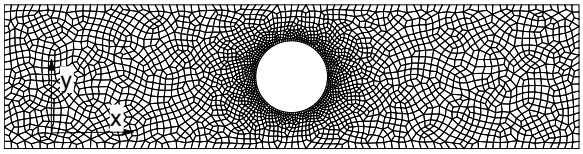

Figure 5: Mesh for channel flow over a cylinder which consits of 3894 elements and has additional refinement near the cylindrical surface.

Boundary Data : We will assume the boundary faces along $y = \pm 0.5$ to be specularly reflecting walls. For the faces along $x = \pm 2.0$, we will assume the incoming distribution function to be given by (8) with the parameters as given in Table 3 therefore, the boundary conditions along these two faces will be given by (66). The boundary conditions along the cylindrical surface will be assumed to be given by the stable set of OBCs, for stationary gas-wall interaction, proposed in [31]; these OBCs are based upon the Maxwell's accommodation model and we will consider the accommodation coefficient to be equal to one. The deviation in temperature of the cylindrical surface upto $\mathscr{O}(\varepsilon)$, $\tilde{\theta}_W$, has been given in Table 3.

Variation of Field Variables : Fig-7(a) shows the streamlines plotted over the pressure contours for $M = 3$ on a zoomed in part of our computational domain ($x \in (-1,1)$). For the part of the computational domain which has not been shown in the plots, the variation of filed variables remains the same as that

Boundary Conditions			
Boundary location	$\tilde{\rho}_{in}$	$\tilde{\theta}_{in}$	$\tilde{\theta}_W$
Left Boundary($x=-2.0$)	1.0	2.0	-
Right Boundary($x=2.0$)	1.0	1.0	-
Cylindrical Surface	-	-	1.0

Table 3: Boundary conditions for the channel flow over a cylinder.

along $x=\pm 1$. Clearly, with the help of the boundary data given in Table 3, we have been successful in creating higher pressure along $x=-2.0$ as compared to along $x=2.0$. This results into a net pressure driven flow from the left boundary to the right. Let $\tilde{v}_t$ be defined as

$$\tilde{v}_t = \tilde{v}_i t_i \quad \text{in} \quad x^2+y^2 = \frac{1}{16} \tag{88}$$

where $\mathbf{t}$ is a tangent vector to the cylindrical surface. Then, $\tilde{v}_t$ represents the tangential velocity along the surface of the cylinder and its variation, along the cylindrical surface, has been shown in fig-6(d). From fig-6(d) we see that the slip velocity is the maximum in magnitude at $\omega=\pi/2$ (see fig-6(d) for definition of ω) which is as expected because $\omega=\pi/2$ corresponds to a point where the cross-section area of the channel is the lowest which results in an accelerated flow in the x-direction. Moreover, in contrast to fig-3(d), we do not see any development of boundary effects which is a result of explicitly prescribing $\tilde{\rho}_{in}$ along the whole open boundary. The velocity profile along the inflow boundary also has only an x-component which does not vary along the y-direction, this is as expected due to the specular walls of the channel. The deviation in pressure $(\tilde{\rho}+\tilde{\theta})$ does not continuously reduce from the inflow and the outflow boundary but rather we observe a significant pressure drop in the wake region of the cylinder.

Due to our boundary data Table 3, the deviation in temperature, $\tilde{\theta}$, reduces continuously from the inflow boundary $x=-2.0$ to the outflow boundary $x=2.0$, see fig-7(b). Moreover, we see a development of a counter Fourier heat flux in the wake region of the cylinder; note that such a heat flux cannot be observed using the classical Stokes or Euler equations [33]. Through a further study which we conducted showed that this counter Fourier heat flux was not an inherent feature of rarefied channel flow across a cylinder but was rather a product of our particular choice of the boundary data in Table 3 and can even be removed by chosing a different set of boundary data. In fig-6(c), we can observe a jump in temperature at the cylinder boundary. Thus, with the help of the Hermite approximation proposed in the present work, and the gas-wall boundary conditions proposed in [31], we have been successful in recovering certain benchmark physical phenomenons which characterise a rarefied gas flow.

Relative Error Variation : A kinetic solution for the present test case is currently unavailable. Therefore, similar to the studies conducted in [2, 20, 41], we will be comparing the error in the solution obtained for three different values of M i.e. $M=3,5$ and 7. These three different values of M then correspond to Grad's-20, 56 and 120 moment equations respectively [8]. The choice of our values of M is motivated from the convergence study conducted in [39] where, for these particular values of M, the error for boundary value problems was found to reduce monotonically as M was increased. Similar to the one-dimensional flow problem, due to its dependence upon all the moments, we study the variation of error in entropy defined as

$$E^{\eta}(\mathbf{x};M_1,M_2) = \int_{\mathbb{R}^3} \eta(f_{M_1} - \Pi_{M_1} f_{M_2}) d\xi \tag{89}$$

where $\eta(f)$ is as defined in (24). We will consider the value of M_2 to be fixed at $M_2=7$ (which will act like a reference solution) and will change M_1 from 3 to 5.

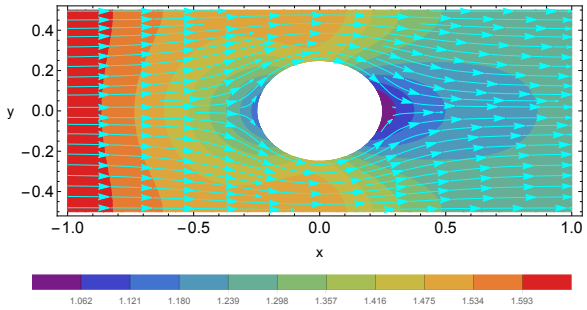

(a) Streamlines plotted over pressure contours for $M = 3$. The aspect ratio of the image is 2.5.

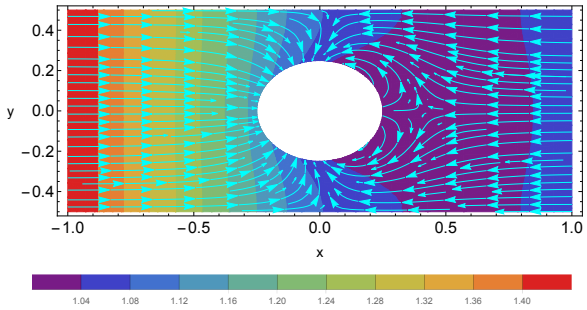

(b) Heat flux vectors plotted over the temperature contours $M = 3$. The aspect ratio of the image is 2.5

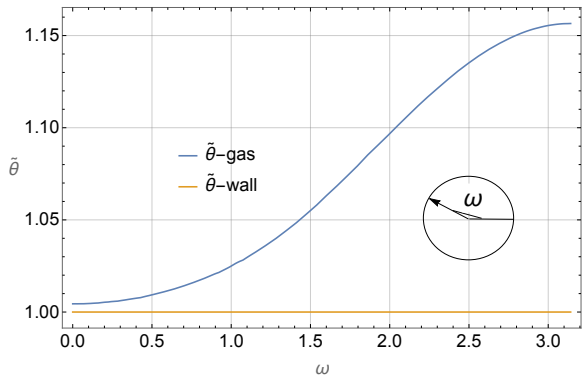

(c) Variation of $\tilde{\theta}$ along the surface of the cylinder.

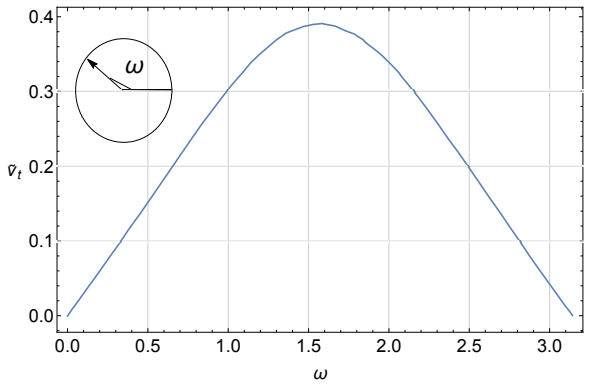

(d) Variation of deviation in tangential velocity ($\tilde{v}_t$) along the surface of the cylinder.

Figure 6: (a) shows the streamlines plotted over the contours for deviation in pressure ($\tilde{\rho} + \tilde{\theta}$). (b) shows the heat flux vectors plotted over the contours for the deviation in temperature ($\tilde{\theta}$). (c) and (d) show the variation of $\tilde{\theta}$ and $\tilde{v}_t$ along the surface of the cylinder respectively.

As we increase the value of M_1, while keeping M_2 fixed, the point-wise value of E^η reduces on the whole computational domain which is a desirable result, see Fig-7(b) and Fig-7(a). Moreover the error in E^η is significantly higher near the boundary of the cylindrical surface which can be a product of the discontinuity of the distribution function near the gas-wall interface. Therefore, it would be desirable to use a physically more accurate model, favourably a moment approximation, near the cylindrical boundary.

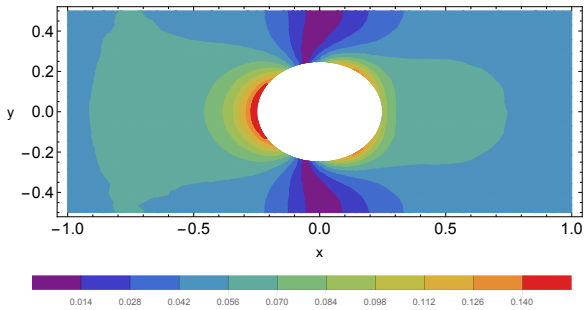

(a) Variation in $E^\eta(\mathbf{x}; 3, 7)$ along the whole computational domain. The aspect ratio of the image is 2.5.

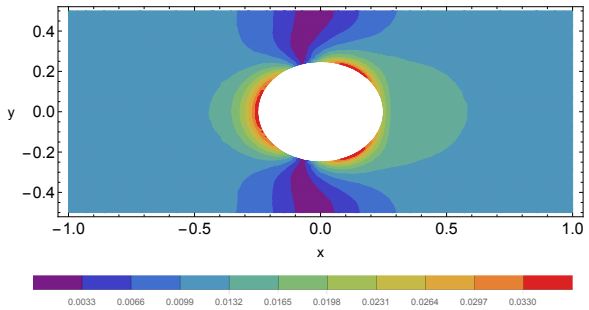

(b) Variation in $E^\eta(\mathbf{x}; 5, 7)$ along the whole computational domain. The aspect ratio of the image is 2.5.

Figure 7: (a) and (b) show the variation in E^η for different values of M_1 and $M_2 = 7$.

6 Discussion

In the present work, we came up with an entropy stable velocity space approximation by first fixing the approximation for h through (22) and then stabilizing the boundary conditions obtained through the continuity of odd fluxes in order to obtain entropy stability but, there could also be other possible methods to obtain an entropy stable approximatino for the linearised BE. One of such methods is the use of a Gauss-Hermite grid in the velocity space which has already been discussed in [30]. Another possible method could be to transform the approximation (22) such that the boundary conditions obtained through the continuity of odd fluxes fulfil the necessary and sufficient condition for the entropy stability formulated in Theorem 3.1. This can be achieved by first developing approximations of the type (22) which have $\mathcal{N}(\mathbf{A}^{oe}) = \mathbf{0}$, such a moment method will already satisfy (58) and might lead to entropy stability with the continuity of odd fluxes. We note that, though there are different ways to construct an entropy stable approximation but, in contrast to (22), they might not lead to a rotationally invariant moment system, a feature of (22) which proves to be helpful while dealing with curved domains [41]. For e.g. the Gauss-Hermite velocity grid based entropy stable discretization proposed in [30] is not rotationally invariant but is equivalent to a discrete velocity scheme. Using certain assumption on the regularity of the kinetic solution, in [30] it was shown that a moment system based upon a Gauss-Hermite grid converges to the true solution of the linearised BE; such a convergence analysis, for the entropy stable Hermite approximation proposed in the present work, is a part of the ongoing research.

The physical accuracy of the approximation (22) depends upon the model of the *Onsager matrix* [28, 34]. In [28, 34], the authors change the coefficients of the *Onsager matrix* appearing in (65) such that the error in a particular moment for a certain benchmark problem reduces. Such a methodology can prove to be computationally expensive as we keep on increasing the value of M (the number of entries in $\mathbf{L}$ are of $\mathcal{O}(M^2)$) or changing the type of the test case. Therefore, it is much more desirable to look for an a priori or an a posteriori error indicator. The main hurdle in the development of such an error indicator could be the discontinuity of the distribution function along the boundary as a result of which even the very high order moments appear in the boundary conditions for the lower order moments. These higher order moments can show up in the error equation through the integral at the boundary. A possible solution to this problem could be the computation of the error with the help of a post-processed reconstructed solution, a methodology which has been used for model adaptivity of hyperbolic conservation laws with relaxations [22]. Such an error estimate can not only help us in improving the *Onsager matrix* but can also be used for an adaptive solution of the BE with the help of moments [2].

A hierarchical numerical discretization of the OBCs in the physical space ($\mathbf{x}$), with the help of a weak boundary implementation [26], can prove to be helpful while having different values of M at different points in the physical space. The entropy stability of the weak boundary implementation depends upon a well defined penalty matrix. A preliminary computational analysis shows that a penalty matrix based upon characteristic splitting, which has been used in the present work, does not preserve the hierarchical nature of the OBCs. The fact that prescribing all the odd moments at the boundary gives us the correct number of boundary conditions indicates an underlying relation between the characteristic variables which come into the domain and the odd variables. Therefore, we speculate that a hierarchical penalty matrix can be developed by exploiting the hierarchical nature of the flux carried by the odd moments; we leave this as a part of our future work.

7 Conclusion

We have developed an entropy stable multi-dimensional Hermite approximation for the linearised Boltzmann equation for bounded position domains involving the inflow and outflow boundaries. We have

shown, without the use of any characteristic splitting, that the use of *Onsager boundary conditions* is both necessary and sufficient for the entropy stability of the Hermite approximation proposed in [17]. With the help of these conditions we have proved that the boundary conditions obtained through the continuity of odd fluxes lead to entropy instability for a large class of the Hermite approximation. Moreover, using the technique of not altering the coefficient of the lower order moments in the continuity of odd fluxes, we come up with a model for the *Onsager matrix*.

Two methodologies to prescribe a particular inflow velocity have been discussed. One of the methodologies relies upon an iterative procedure and considers the complete incoming distribution function to be a given quantity (or independent of the solution). The entropy stability of such a method trivially follows for both the linearised Boltzmann equation and its Hermite approximation. The other methodology relied upon treating the density of the incoming distribution function as a free parameter and then computing it such that the velocity along the inflow remains constant. This methodology lead to entropy instability for both the linearised Boltzmann equation and its Hermite approximation. Since the second methodology is cheaper to implement than the first one, an entropy stabilization has been proposed for the same; the accuracy of the proposed stabilization has been studied with the help of a benchmark problem.

The entropy stable Hermite approximation has been found to converge to the kinetic solution, with an order of convergence close to one, for a one-dimensional flow problem with acceptable accuracy. Furthermore, the proposed approximation has been used to study channel flow over a cylinder which demonstrates its capability in capturing certain benchmark physical phenomenons occurring in rarefied gas flows.

8 Appendix

8.1 Ordering for $\beta^{(i)}$

We will now present an example for the ordering of $\beta^{(i)}$ used in the present work. Consider $M = 3$ in (22) then our resulting moment system will correspond to the ordered moment theory $G20$ (Grad's-20) [8]. For this particular value of M, we will consider the following ordering for the set $\mathscr{S}$ which contains all the tuples $\beta^{(i)}$

$$\mathscr{S} = \Bigg(\underbrace{(0,0,0)}_{0\text{ th-order}}, \underbrace{(1,0,0),(0,1,0),(0,0,1)}_{1\text{ st-order}}, \underbrace{(2,0,0),(1,1,0),(1,0,1),(0,2,0),(0,1,1),(0,0,2)}_{2\text{ nd-order}}, \\ \underbrace{(3,0,0),(2,1,0),(2,0,1),(1,2,0),(1,1,1),(1,0,2),(0,3,0),(0,2,1),(0,1,2),(0,0,3)}_{3\text{ rd-order}} \Bigg) \tag{90}$$

Let $\mathscr{S}^o$ and $\mathscr{S}^e$ represent a set containing all the tuples $\beta^{(i,o)}$ and $\beta^{(i,e)}$ respectively, then we have

$$\mathscr{S}^o = \Bigg(\underbrace{(1,0,0)}_{1\text{ st-order}}, \underbrace{(1,1,0),(1,0,1)}_{2\text{ nd-order}}, \underbrace{(3,0,0),(1,2,0),(1,1,1),(1,0,2)}_{3\text{ rd-order}} \Bigg) \tag{91}$$

$$\mathscr{S}^e = \mathscr{S} - \mathscr{S}^o = \Bigg(\underbrace{(0,0,0)}_{0\text{ th-order}}, \underbrace{(0,1,0),(0,0,1)}_{1\text{ st-order}}, \underbrace{(2,0,0),(0,2,0),(0,1,1),(0,0,2)}_{2\text{ nd-order}}, \underbrace{(2,1,0),(2,0,1),(0,3,0),(0,2,1),(0,1,2),(0,0,3)}_{3\text{ rd-order}} \Bigg) \tag{92}$$

We see that the number of odd variables are strictly less than the number of even variables in general.

8.2 Proof of Theorem-3.1

Theorem. Let a quadratic form $\mathscr{M}$ be defined as

$$\mathscr{M} = -\left((\alpha^q)^T \mathbf{M}^T \mathbf{A} \alpha^q + \mathbf{g}^T \mathbf{A} \alpha^q \right) \tag{93}$$

where $\mathbf{A} \in \mathbb{R}^{p \times q}$ $(p < q)$ is a constant matrix, $rank(\mathbf{A}) = p$ and $\mathbf{g} \in \mathbb{R}^p$ is independent of α^q. Let κ be some factor independent of α^q then, $\mathscr{M} \leq \kappa$ for all $\alpha^q \in \mathbb{R}^q$, if and only if

$$\mathbf{M} = \mathbf{L}\mathbf{A} \quad \text{and} \quad \mathbf{g} \in range(sym(\mathbf{L})) \tag{94}$$

where $\mathbf{L}$ is a constant positive semi-definite matrix and $sym(\mathbf{L})$ is the symmetric part of $\mathbf{L}$.

Proof. First we prove our claim in one direction i.e. we assume $\mathbf{M} = \mathbf{L}\mathbf{A}$ with $\mathbf{L}$ being a constant positive semi-definite matrix and $\mathbf{g} \in range(sym(\mathbf{L}))$ and show that $\mathscr{M} \leq \kappa$. Replacing such an $\mathbf{M}$ into $\mathscr{M}$ given in (93), we obtain

$$\begin{aligned}
\mathscr{M} &= -\left[(\mathbf{A}\alpha^q)^T \mathbf{L}^T \mathbf{A}\alpha^q + \mathbf{g}^T \mathbf{A}\alpha^q \right] && \text{(95a)} \\
&= -\left[(\tilde{\mathbf{x}} + \tilde{\mathbf{g}})^T sym(\mathbf{L}) (\tilde{\mathbf{x}} + \tilde{\mathbf{g}}) - \tilde{\mathbf{g}}^T sym(\mathbf{L}) \tilde{\mathbf{g}} \right], \quad (\text{with } \tilde{\mathbf{x}} = \mathbf{A}\alpha^q, \tilde{\mathbf{g}} = \frac{1}{2} sym(\mathbf{L})^\dagger \mathbf{g}) && \text{(95b)} \\
&\leq \tilde{\mathbf{g}}^T sym(\mathbf{L}) \tilde{\mathbf{g}}, \quad (\because sym(\mathbf{L}) \geq 0) && \text{(95c)}
\end{aligned}$$

where $sym(\mathbf{L})^\dagger$ is the pseudo-inverse of $sym(\mathbf{L})$. Identifying κ as $\tilde{\mathbf{g}}^T sym(\mathbf{L}) \tilde{\mathbf{g}}$ proves our claim. Note that we can choose such a $\tilde{\mathbf{g}}$ because $\mathbf{g} \in range(sym(\mathbf{L}))$.

Now we prove our claim in the other direction, we assume that $\mathscr{M}$ is bounded as $\mathscr{M} \leq \kappa$ and show that $\mathbf{M} = \mathbf{L}\mathbf{A}$ with $\mathbf{L} \geq 0$ and $\mathbf{g} \in range(sym(\mathbf{L}))$. Let $\mathscr{R} \subset \mathbb{R}^q$ be defined as $\mathscr{R} = \{\lambda \alpha_0^q + \tilde{\alpha}^q | \lambda \in \mathbb{R}\}$ where $\alpha_0^q \in \mathscr{N}(\mathbf{A})$ and $\tilde{\alpha}^q \notin \mathscr{N}(\mathbf{A})$ are two non-zero fixed vectors; $\mathscr{N}(\mathbf{A}) \neq \{\mathbf{0}\}$ is the null space of $\mathbf{A}$. Of course, $\mathscr{M}$ should also be bounded on $\mathscr{R}$. Substituting a α^q from $\mathscr{R}$ into $\mathscr{M}$ in (93), we obtain

$$\Gamma(\lambda) = \mathscr{M} = -\left[(\mathbf{M}\tilde{\alpha}^q)^T \mathbf{A}\tilde{\alpha}^q + \lambda \left(\mathbf{M}\alpha_0^q\right)^T \mathbf{A}\tilde{\alpha}^q + \mathbf{g}^T \mathbf{A}\tilde{\alpha}^q \right] \tag{96}$$

which should be bounded from above independently of λ. Since $\tilde{\alpha}^q$, α_0^q and $\mathbf{g}$ are fixed vectors, $\Gamma(\lambda) \leq \kappa$ only if $\mathbf{M}\alpha_0^q = \mathbf{0}$. Which implies $\mathscr{N}(\mathbf{A}) \subseteq \mathscr{N}(\mathbf{M})$ or $\mathbf{M} = \mathbf{L}\mathbf{A}$, where $\mathbf{L} \in \mathbb{R}^{p \times p}$ is some constant matrix. Replacing such an $\mathbf{M}$ into $\mathscr{M}$ in (93), we will obtain the same expression as (95a). To prove our claim, we now need to show that $\mathbf{L} \geq 0$ and $\mathbf{g} \in range(sym(\mathbf{L}))$. Let us assume that $\mathbf{L}$ is not positive semi-definite then, $sym(\mathbf{L})$ will have an eigenvector $\mathbf{v}^-$ with a negative eigenvalue λ^-. Choosing $\mathbf{A}\alpha^q = \gamma \mathbf{v}^-$ (which is always possible since $\mathbf{A}$ has full rank) in (95a) with $\gamma \in \mathbb{R}$, we will obtain $\mathscr{M} = -\gamma^2 \lambda^- \|\mathbf{v}^-\|^2 - \gamma \mathbf{g}^T \mathbf{v}^-$ which is not bounded from above independently of γ. This implies that $\mathbf{L} \geq 0$.

Any vector $\mathbf{g}$ can be expressed as $\mathbf{g} = \mathbf{g}_0 + \mathbf{g}_1$ where $\mathbf{g}_0 \notin range(sym(\mathbf{L}))$ and $\mathbf{g}_1 \in range(sym(\mathbf{L}))$.

Replacing the decomposition of $\mathbf{g}$ into (95a) we obtain

$$\mathscr{M} \leq \frac{1}{4}\mathbf{g}_1^T sym(\mathbf{L})^{\dagger}\mathbf{g}_1 - \mathbf{g}_0^T\mathbf{A}\alpha^q, \quad (\because sym(\mathbf{L}) \geq 0) \tag{97}$$

which can be bounded independently of α^q only if $\mathbf{g}_0 = 0$. This proves our claim. □

8.3 Proof of Lemma-3.1

Lemma. Assuming $M \geq 2$ and $d \leq 3$, the boundary conditions, given in (55), obtained from the continuity of odd fluxes satisfy (58) if and only if $d = 1$ in (2) and M is odd in (22).

Proof. For $d = 1$ and M odd, $n_o = n_e$ and $\tilde{\mathbf{A}}^{(oe)} = 0$ in (47) which implies $\mathscr{N}(\mathbf{A}^{oe}) = \{\mathbf{0}\}$ ($det(\hat{\mathbf{A}}^{(oe)}) \neq 0$) [31]. Therefore, the condition in (58) is satisfied. We will assume $d = 3$ for further discussion, the results for any other $d < 3$ trivially follow by removing the contributions from extra dimensions. The total number of odd n_o and even n_e moments are related to M as

$$\begin{gathered} n_e = \sum_{r=0}^{M}\sum_{i=0}^{\lfloor \frac{r}{2} \rfloor}[r+1-2i], \quad n_o = \sum_{r=0}^{M}\sum_{i=0}^{\lceil \frac{r}{2} \rceil - 1}[r-2i] \\ n_e - n_o = \sum_{i=0}^{\lfloor \frac{M}{2} \rfloor}[M+1-2i] \end{gathered} \tag{98}$$

where $\lfloor n \rfloor$ and $\lceil n \rceil$ represent the smallest (or equal to) and the largest (or equal to) integer than n respectively. It is easy to check that $n_e - n_o$ is equal to the total number of even basis functions which have $|\beta^{(i,e)}| = M$. Trivially $n_o < n_e$ and therefore $\mathscr{N}(\mathbf{A}^{oe}) \neq \{\mathbf{0}\}$. We now show that there belongs atleast one non-zero element in $\mathscr{N}(\mathbf{A}^{oe})$ which is not in $\mathscr{N}(\mathbf{M}^{(in)})$. Let $\mathbf{x}^e \in \mathscr{N}(\mathbf{A}^{oe})$ and let $\tilde{\mathbf{x}}^e$ represent the last $n_e - n_o$ entries of $\mathbf{x}^e$. Then due to (47), $\mathbf{x}^e$ will be given as

$$\mathbf{x}^e = span\left\{ \begin{pmatrix} -\left(\hat{\mathbf{A}}^{(oe)}\right)^{-1}\tilde{\mathbf{A}}^{(oe)}\tilde{\mathbf{x}}^e \\ \tilde{\mathbf{x}}^e \end{pmatrix} \right\} \tag{99}$$

where $\tilde{\mathbf{x}}^e \in \mathbb{R}^{n_e - n_o}$ and will be assumed to be non-zero.

We will now choose $\tilde{\mathbf{x}}^e = (\gamma, 0 \ldots 0)^T$ ($\gamma \in \mathbb{R}/\{0\}$) and define $\hat{f}^e = f_0 \sum_{|\beta^{(i,e)}| \leq M} x_i^e \psi_{\beta^{(i,e)}}$. Then, the coefficient γ will correspond to the first even basis with $|\beta^{(i,e)}| = M$ i.e. the basis given by

$$\psi_{\beta^{(i,e)}} = \begin{cases} He_{M-1}\left(\frac{\xi_1}{\sqrt{\theta_0}}\right) He_1\left(\frac{\xi_2}{\sqrt{\theta_0}}\right) He_0\left(\frac{\xi_3}{\sqrt{\theta_0}}\right), & M \text{ odd} \\ He_M\left(\frac{\xi_1}{\sqrt{\theta_0}}\right) He_0\left(\frac{\xi_2}{\sqrt{\theta_0}}\right) He_0\left(\frac{\xi_3}{\sqrt{\theta_0}}\right), & M \text{ even} \end{cases} \tag{100}$$

From the definition of $\mathbf{A}^{oe}$ in (46), we know that

$$A_{ij}^{oe} x_j^e = \int_{\mathbb{R}^d} \psi_{\beta^{(i,o)}} \xi_1 \hat{f}^e d\xi = 0, \quad i \in \{0, \ldots n_o - 1\}, \tag{101}$$

which implies $\xi_1 \hat{f}^e \in span\{\psi_{\beta^{(i,o)}}\}$ with $|\beta^{(i,o)}| > M$. Due to the basis corresponding to γ (100) and the

recursion relations of the Hermite polynomials (16b), $\xi_1 \hat{f}^e$ can be given as

$$\xi_1 \hat{f}^e = \begin{cases} \sqrt{\theta_0}\gamma\sqrt{M} He_M\left(\frac{\xi_1}{\sqrt{\theta_0}}\right) He_1\left(\frac{\xi_2}{\sqrt{\theta_0}}\right) He_0\left(\frac{\xi_3}{\sqrt{\theta_0}}\right) f_0, & M \text{ odd} \\ \sqrt{\theta_0}\gamma\sqrt{M+1} He_{M+1}\left(\frac{\xi_1}{\sqrt{\theta_0}}\right) He_0\left(\frac{\xi_2}{\sqrt{\theta_0}}\right) He_0\left(\frac{\xi_3}{\sqrt{\theta_0}}\right) f_0, & M \text{ even} \end{cases} \tag{102}$$

In order to show that $\mathbf{x}^e \notin \mathcal{N}(\mathbf{M}^{(in)})$, we express $\mathbf{M}^{(in)}\mathbf{x}^e$ as $M_{ij}^{(in)} x_j^e = \int_{\mathbb{R}^{d-1}} \int_{\xi_1>0} \psi_{\beta^{(i,o)}} \hat{f}^e d\xi$. Choosing

$$\psi_{\beta^{(i,o)}} = \begin{cases} He_1\left(\frac{\xi_1}{\sqrt{\theta_0}}\right) He_1\left(\frac{\xi_2}{\sqrt{\theta_0}}\right) He_0\left(\frac{\xi_3}{\sqrt{\theta_0}}\right), & M \text{ odd} \\ He_1\left(\frac{\xi_1}{\sqrt{\theta_0}}\right) He_0\left(\frac{\xi_2}{\sqrt{\theta_0}}\right) He_0\left(\frac{\xi_3}{\sqrt{\theta_0}}\right), & M \text{ even} \end{cases} \tag{103}$$

we obtain

$$\int_{\mathbb{R}^{d-1}} \int_{\xi_1>0} \psi_{\beta^{(i,o)}} \hat{f}^e d\xi = \begin{cases} \gamma\sqrt{M} \int_{\xi_1>1} He_M\left(\frac{\xi_1}{\sqrt{\theta_0}}\right) f_0 d\xi = \rho_0 \gamma (-1)^{(M-1)/2} \frac{(M-2)!!}{\sqrt{2\pi(M-1)!}}, & M \text{ odd} \\ \gamma\sqrt{M+1} \int_{\xi_1>0} He_{M+1}\left(\frac{\xi_1}{\sqrt{\theta_0}}\right) f_0 d\xi = \rho_0 \gamma (-1)^{M/2} \frac{(M-1)!!}{\sqrt{2\pi(M)!}}, & M \text{ even} \end{cases} \tag{104}$$

where we have used $He_1\left(\xi_1/\sqrt{\theta_0}\right) = \xi_1/\sqrt{\theta_0}$. Note that we can chose such an $\psi_{\beta^{(i,o)}}$, as given in (103), because we have restricted $M \geq 2$ (ensures $\mathscr{I} \subset \mathscr{V}_M$). Since the expression in (104) will be non-zero for any $\gamma \neq 0$, this proves our claim. □

8.4 Proof of Theorem-3.2

Theorem. The matrix $\mathbf{L}^{(in)}$ given by (65) is s.p.d.

Proof. If $\mathbf{L}^{(in)}$ is *spd* then $\hat{\mathbf{P}} = \left(\hat{\mathbf{A}}^{oe}\right)^T \mathbf{L}^{(in)} \hat{\mathbf{A}}^{oe} = \left(\hat{\mathbf{A}}^{oe}\right)^T \hat{\mathbf{M}}^{(in)}$ should also be *spd* (recall $\hat{\mathbf{A}}^{(oe)}$ is invertible). Using the expression for $\hat{\mathbf{M}}^{(in)}$ from (56a), $\hat{\mathbf{P}}$ can be written as

$$\begin{aligned}
\hat{P}_{ik} =& \hat{\mathbf{A}}_{ji}^{oe} \hat{\mathbf{M}}_{jk}^{(in)} \\
=& \frac{1}{\rho_0} \hat{\mathbf{A}}_{ji}^{oe} \int_{\xi_1>0} \psi_{\beta^{(j,o)}} \psi_{\beta^{(k,e)}} f_0 d\xi \\
=& \frac{1}{\rho_0} \left\langle \psi_{\beta^{(j,o)}} f_0, \xi_1 \psi_{\beta^{(i,e)}} f_0 \right\rangle_{\mathscr{H}} \int_{\xi_1>0} \psi_{\beta^{(j,o)}} \psi_{\beta^{(k,e)}} f_0 d\xi \\
=& \sqrt{\theta_0} \left(\sqrt{m_1^{(j,o)}+1}\, \delta_{m_1^{(j,o)}+1, m_1^{(i,e)}} + \sqrt{m_1^{(j,o)}}\, \delta_{m_1^{(j,o)}-1, m_1^{(i,e)}} \right) \prod_{p=2}^{d} \delta_{m_p^{(j,o)}, m_p^{(i,e)}} \\
& \times \int_{\xi_1>0} \psi_{\beta^{(j,o)}} \psi_{\beta^{(k,e)}} f_0 d\xi \\
=& \sqrt{\theta_0} \left(\sqrt{m_1^{(j,o)}+1}\, \delta_{m_1^{(j,o)}+1, m_1^{(i,e)}} + \sqrt{m_1^{(j,o)}}\, \delta_{m_1^{(j,o)}-1, m_1^{(i,e)}} \right) \\
& \times \int_{\xi_1>0} \left(He_{m_1^{(j,o)}}\left(\frac{\xi_1}{\sqrt{\theta_0}}\right) \prod_{p=2}^{d} He_{m_p^{(i,e)}}\left(\frac{\xi_p}{\sqrt{\theta_0}}\right) \right) \psi_{\beta^{(k,e)}} f_0 d\xi
\end{aligned}$$

$$
\begin{aligned}
&= \sqrt{\theta_0} \int_{\xi_1>0} \left(\sqrt{m_1^{(i,e)}} He_{m_1^{(i,e)}-1}\left(\frac{\xi_1}{\sqrt{\theta_0}}\right) + \sqrt{m_1^{(i,e)}+1} He_{m_1^{(i,e)}+1}\left(\frac{\xi_1}{\sqrt{\theta_0}}\right)\right) \\
&\times \prod_{p=2}^{d} He_{m_p^{(i,e)}}\left(\frac{\xi_p}{\sqrt{\theta_0}}\right) \psi_{\beta^{(k,e)}} f_0 d\xi \\
&= \int_{\xi_1>0} \psi_{\beta^{(i,e)}} \xi_1 \psi_{\beta^{(k,e)}} f_0 d\xi
\end{aligned} \tag{105}
$$

The above expression is symmetric with respect to i and k. In writing the above relation we have used the orthogonality (16a) and the recursion relation (16b) of the Hermite polynomials. Let the quadratic form of $\hat{\mathbf{P}}$ be represented by κ then

$$
\kappa = \hat{x}_i \hat{P}_{ik} \hat{x}_k. \tag{106}
$$

where $\hat{\mathbf{x}} \in \mathbb{R}^{n^o}$. Let $\bar{f}$ be a function such that

$$
\bar{f}(\mathbf{x},\xi,t) = \sum_{i=0}^{n_o} \hat{x}_i \psi_{\beta^{(i,e)}} f_0(\xi) \quad \forall \xi_1 \in \mathbb{R}^+. \tag{107}
$$

Then κ reads

$$
\kappa = \hat{x}_i \left(\int_{\xi_1>0} \psi_{\beta^{(i,e)}} \xi_1 \psi_{\beta^{(k,e)}} f_0 d\xi \right) \hat{x}_k = \int_{\xi_1>0} \hat{x}_i \psi_{\beta^{(i,e)}} \xi_1 \psi_{\beta^{(k,e)}} \hat{x}_k f_0 d\xi = \int_{\xi_1>0} \bar{f}^2 \xi_1 f_0^{-1} d\xi \tag{108}
$$

The integrals in the above expression will be bounded because $\bar{f} \in F$. The above expression implies $\kappa > 0$ for all non-zero $\hat{\mathbf{x}}$. Hence $\hat{\mathbf{P}}$ is *s.p.d* and so is $\mathbf{L}^{(in)}$. □

8.5 Proof of Lemma-4.1

Lemma. Using *Method1*, we obtain the entropy estimate

$$
d_t S(f) \leq H(t) - \frac{2}{\beta} \left(\oint_{\partial\Omega} \hat{v}_n \left[\int_{\mathbb{R}^{d-1}} \int_{\xi_n>0} \xi_n f_e d\xi \right] ds \right) \tag{109}
$$

where f_e is the even part of f with respect to ξ_n and $\beta = \int_{\mathbb{R}^{d-1}} \int_{\xi_n>0} \xi_n f_0(\xi) d\xi$.

Proof. For *Method1*, we can compute $\tilde{\rho}^+$ from (70a)

$$
\frac{\tilde{\rho}^+}{\rho_0} = \frac{1}{f_0(\xi)} \left(\int_{\mathbb{R}^{d-1}} \int_{\xi_n'>0} \omega(\xi,\xi') f(\mathbf{x},\xi',t) d\xi' + g(\mathbf{x},\xi,t) \right) \tag{110}
$$

where $g(\mathbf{x},\xi,t)$ and $\omega(\xi,\xi')$ are given as

$$
\begin{aligned}
\beta = \int_{\mathbb{R}^{d-1}} \int_{\xi_n>0} \xi_n f_0(\xi) d\xi, \quad g(\mathbf{x},\xi,t) = -\frac{\hat{v}_n(\mathbf{x},t) f_0(\xi)}{\beta}, \quad \mathbf{x} \in \partial\Omega^+ \\
\omega(\xi,\xi') = \frac{\xi_n' f_0(\xi)}{\beta}, \quad \xi_n' \in \mathbb{R}^+
\end{aligned} \tag{111}
$$

We note that $\omega(\xi,\xi')$ is positive for $\xi_n' \in \mathbb{R}^+$. Due to (110), the assumed bound in (33) can no more be used ($H(t)$ will not be independent of the solution) to obtain entropy stability. Using the relation for $\tilde{\rho}^+$,

the distribution function f_{in} along $\partial\Omega^+$ can be given as

$$f_{in}(\mathbf{x},\xi) = \int_{\mathbb{R}^{d-1}}\int_{\xi_n'>0} \omega(\xi,\xi')f(\mathbf{x},\xi')d\xi' + g(\mathbf{x},\xi) \quad \text{in} \quad \partial\Omega^+\times\mathbb{R}^- \tag{112}$$

where we have hidden the dependencies on t for brevity. Cauchy-Schwartz inequality provides us [30]

$$(f_{in}(\xi)-g(\xi))^2 \leq f_0(\xi)\int_{\mathbb{R}^{d-1}}\int_{\xi_n'>0}\omega(\xi,\xi')\frac{f^2(\xi')}{f_0(\xi')}d\xi'. \tag{113}$$

where the integral exists because we have assumed $f\in\mathscr{H}$. Multiplying the above inequality by $\xi_n<0$ and integrating over ξ, we obtain

$$\int_{\mathbb{R}^{d-1}}\int_{\xi_n<0}\xi_n f_0^{-1}(f_{in}(\xi)-g(\mathbf{x},\xi))^2 d\xi \geq \int_{\mathbb{R}^{d-1}}\int_{\xi_n<0}\xi_n\int_{\mathbb{R}^{d-1}}\int_{\xi_n'>0}\omega(\xi,\xi')\frac{f^2(\xi')}{f_0(\xi')}d\xi' d\xi \tag{114}$$

Let us now look into the entropy flux at a particular point along the boundary $\partial\Omega^+$

$$\begin{aligned}\langle\xi_n f,f\rangle_{\mathscr{H}} &= \int_{\mathbb{R}^{d-1}}\int_{\xi_n<0}\xi_n\frac{f_{in}^2(\xi)}{f_0}d\xi + \int_{\mathbb{R}^{d-1}}\int_{\xi_n>0}\xi_n\frac{f^2(\xi)}{f_0}d\xi, \quad \mathbf{x}\in\partial\Omega^+\\ &= \int_{\mathbb{R}^{d-1}}\int_{\xi_n<0}\xi_n(f_{in}-g)^2 f_0^{-1}d\xi + \int_{\mathbb{R}^{d-1}}\int_{\xi_n<0}\xi_n\frac{g(\xi)}{f_0(\xi)}(2f_{in}-g(\xi))d\xi\\ &\quad + \int_{\mathbb{R}^{d-1}}\int_{\xi_n>0}\xi_n\frac{f^2(\xi)}{f_0}d\xi\end{aligned} \tag{115}$$

Using (114) and $\int_{\mathbb{R}^{d-1}}\int_{\xi_n<0}\xi_n\omega(\xi,\xi')d\xi = -\xi_n'$ in the above relation, we obtain

$$\begin{aligned}\langle\xi_n f,f\rangle_{\mathscr{H}} &\geq \int_{\mathbb{R}^{d-1}}\int_{\xi_n<0}\xi_n\frac{g(\xi)}{f_0(\xi)}(2f_{in}-g(\xi))d\xi\\ &= -\frac{2\hat{v}_n}{\beta}\int_{\mathbb{R}^{d-1}}\int_{\xi_n<0}\xi_n f(\xi)d\xi + \frac{\hat{v}_n^2}{\beta} \quad (\because f(\xi)=f_{in} \quad \forall\xi_n<0)\end{aligned} \tag{116}$$

To simplify the bound further, let f_o and f_e represent the odd and the even parts of f, with respect to ξ_n, respectively. This leads to

$$\begin{aligned}\langle\xi_n f,f\rangle_{\mathscr{H}} &\geq -\frac{2\hat{v}_n}{\beta}\int_{\mathbb{R}^{d-1}}\int_{\xi_n<0}\xi_n f_o d\xi - \frac{2\hat{v}_n}{\beta}\int_{\mathbb{R}^{d-1}}\int_{\xi_n<0}\xi_n f_e d\xi + \frac{\hat{v}_n^2}{\beta}\\ &= \frac{2\hat{v}_n}{\beta}\int_{\mathbb{R}^{d-1}}\int_{\xi_n>0}\xi_n f_e d\xi, \quad \left(\because 2\int_{\mathbb{R}^{d-1}}\int_{\xi_n>0}\xi_n f_o d\xi = \int_{\mathbb{R}^d}\xi_n f_o d\xi = \int_{\mathbb{R}^d}\xi_n f d\xi = \hat{v}_h\right)\end{aligned} \tag{117}$$

At the outflow boundary ($\partial\Omega^-$), we don't need to do anything special i.e. we simply need to prescribe a $\tilde{\rho}^-$ independently of the solution. Therefore, we can bound the entropy flux along $\partial\Omega^-$ corresponding to $\xi_n<0$ as

$$-\oint_{\partial\Omega^-}\int_{\mathbb{R}^d}\xi_n f_{in}^2 f_0^{-1}d\xi ds \leq H(t) < \infty, \quad \mathbf{x}\in\partial\Omega^- \tag{118}$$

If we now revisit the entropy estimate in (30), then using the bounds for the entropy flux obtained above, we have

$$d_t S(f) \leq H(t) - \frac{2}{\beta}\left(\oint_{\partial\Omega}\hat{v}_n\left[\int_{\mathbb{R}^{d-1}}\int_{\xi_n>0}\xi_n f_e d\xi\right]ds\right) \tag{119}$$

which proves our claim. □

8.6 Proof of Lemma-4.2

Lemma. Assume the deviation in density and temperature to be given quantities along the outflow boundary $\partial\Omega_1^-$. Then, by prescribing the boundary conditions in (75), with $\mathbf{L}^+$ being replaced by $\mathbf{L}^+_{reg}$, along $\partial\Omega_1^+$ and the boundary conditions of the type (66) along the outflow boundary $\partial\Omega_1^-$ we obtain

$$d_t S(f_M) \leq \mathscr{T}(t,\kappa) \tag{120}$$

where $\mathscr{T}(t,\kappa)$ is $\mathscr{O}(\kappa^{-1})$.

Proof. The boundary conditions along $\partial\Omega_1^+$ and $\partial\Omega_1^-$, which follow from (75) and (66) respectively, can be generically given as

$$\begin{aligned} \alpha^o &= \mathbf{L}^+_{reg}\mathbf{A}^{oe}\alpha^e + \mathbf{g}^+, \quad \text{in} \quad \partial\Omega_1^+ \\ \alpha^o &= \mathbf{L}^-\mathbf{A}^{oe}\alpha^e + \mathbf{g}^-, \quad \text{in} \quad \partial\Omega_1^- \end{aligned} \tag{121}$$

where $\mathbf{L}^+_{reg}$ and $\mathbf{L}^-$ are as given in (78) and (65) respectively; moreover, they are both *s.p.d.* Using the boundary conditions given in (121), the entropy flux (45) along the boundary $\partial\Omega_1$ can be given as

$$\int_{\partial\Omega_1}\int_{\mathbb{R}^d}\phi^{(1)}(f_M)d\xi ds = \int_{\partial\Omega_1^+}\phi_1^+ ds + \int_{\partial\Omega_1^-}\phi_1^- ds \tag{122}$$

where

$$\phi_1^+ = (\mathbf{A}^{oe}\alpha^e)^T\mathbf{L}^+_{reg}\mathbf{A}^{oe}\alpha^e + (\mathbf{g}^+)^T\mathbf{A}^{oe}\alpha^e, \quad \phi_1^- = (\mathbf{A}^{oe}\alpha^e)^T\mathbf{L}^-\mathbf{A}^{oe}\alpha^e + (\mathbf{g}^-)^T\mathbf{A}^{oe}\alpha^e. \tag{123}$$

Using the s.p.d nature of $\mathbf{L}^-$ and $\mathbf{L}^+_{reg}$, we can easily find

$$\phi_1^- \geq -\frac{1}{4}(\mathbf{g}^-)^T(\mathbf{L}^-)^{-1}\mathbf{g}^-, \quad \phi_1^+ \geq -\frac{1}{4}(\mathbf{g}^+)^T(\mathbf{L}^+_{reg})^{-1}\mathbf{g}^+. \tag{124}$$

In (124), the matrix $(\mathbf{L}^-)^{-1}$ is independent of κ whereas $(\mathbf{L}^+_{reg})^{-1}$ is $\mathscr{O}(\kappa^{-1})$ due to the structure

$$(\mathbf{L}^+_{reg})^{-1} = \begin{pmatrix} \kappa^{-1} & \mathbf{0} \\ \mathbf{0} & \bar{\mathbf{L}}^{-1} \end{pmatrix} \tag{125}$$

and hence, the lower bound for ϕ_1^+ is $\mathscr{O}(\kappa^{-1})$ for every non-zero $\hat{v}_1$. Replacing the bounds for ϕ_1^+ and ϕ_1^- into (122) and substituting the resulting entropy flux into (36), we obtain

$$\partial_t S(f_M) \leq \frac{1}{4}\int_{\partial\Omega_1^+}(\mathbf{g}^+)^T(\mathbf{L}^+_{reg})^{-1}\mathbf{g}^+ ds + \frac{1}{4}\int_{\partial\Omega_1^-}(\mathbf{g}^-)^T(\mathbf{L}^-)^{-1}\mathbf{g}^- ds. \tag{126}$$

Using the initial conditions from (7) and combining all the known factors into one time and κ dependent function, $\mathscr{T}$, we obtain

$$d_t S(f_M) \leq \mathscr{T}(t,\kappa) \tag{127}$$

where $\mathscr{T}(t,\kappa)$ will be $\mathscr{O}(\kappa^{-1})$ due to (78).

□

References

[1] Abdelmalik, M. and van Brummelen, E. (2016a). An entropy stable discontinuous galerkin finite-element moment method for the boltzmann equation. *Computers & Mathematics with Applications*, 72(8):1988 – 1999. Finite Elements in Flow Problems 2015.

[2] Abdelmalik, M. and van Brummelen, E. (2017). Error estimation and adaptive moment hierarchies for goal-oriented approximations of the boltzmann equation. *Computer Methods in Applied Mechanics and Engineering*, 325(Supplement C):219 – 239.

[3] Abdelmalik, M. R. A. and van Brummelen, E. H. (2016b). Moment closure approximations of the boltzmann equation based on ϕ-divergences. *Journal of Statistical Physics*, 164(1):77–104.

[4] Akhlaghi, H., Roohi, E., and Stefanov, S. (2012). A new iterative wall heat flux specifying technique in DSMC for heating/cooling simulations of MEMS/NEMS. *International Journal of Thermal Sciences*, 59:111 – 125.

[5] Bangerth, W., Davydov, D., Heister, T., Heltai, L., Kanschat, G., Kronbichler, M., Maier, M., Turcksin, B., and Wells, D. (2016). The `deal.II` library, version 8.4. *Journal of Numerical Mathematics*, 24.

[6] B.Gustafsson, H.O.Kriess, and J.Olinger (1995). *Time Dependent Problems and Difference Methods*. John Wiley and Sons, Inc.

[7] Bird, G. A. (1995). *Molecular gas dynamics and the direct simulation of gas flows*. Oxford : Clarendon Press, repr. (with corrections) edition.

[8] Cai, Z. and Li, R. (2010). Numerical regularized moment method of arbitrary order for boltzmann-bgk equation. *SIAM Journal on Scientific Computing*, 32(5):2875–2907.

[9] Cai, Z. and Torrilhon, M. (2017). Numerical simulation of microflows using moment methods with linearized collision operator. *Journal of Scientific Computing*.

[10] Cercignani, C. (1988). *The Boltzmann Equation and Its Applications*. Springer, 67 edition.

[11] Christian, R. (2002). Numerical methods for the semiconductor boltzmann equation based on spherical harmonics expansions and entropy discretizations. *Transport Theory and Statistical Physics*, 31(4-6):431–452.

[12] Dafermos, C. (2010). *Hyperbolic Conservation Laws in Continuum Physics*. Springer-Verlag,Berlin.

[13] Fan, Y., Koellermeier, J., Li, J., Li, R., and Torrilhon, M. (2016). Model reduction of kinetic equations by operator projection. *Journal of Statistical Physics*, 162(2):457–486.

[14] Gassner, G. J. (2013). A skew-symmetric discontinuous galerkin spectral element discretization and its relation to sbp-sat finite difference methods. *SIAM Journal on Scientific Computing*, 35(3):A1233–A1253.

[15] Geuzaine, C. and Remacle, J.-F. (2009). Gmsh: A 3-d finite element mesh generator with built-in pre- and post-processing facilities. *International Journal for Numerical Methods in Engineering*, 79(11):1309–1331.

[16] Grad, H. (1949). Note on N-dimensional hermite polynomials. *Communications on Pure and Applied Mathematics*, 2(4):325–330.

[17] Grad, H. (1949). On the kinetic theory of rarefied gases. *Communications on Pure and Applied Mathematics*, 2(4):331–407.

[18] Grad, H. (1965). On Boltzmann's H-theorem. *Journal of the Society for Industrial and Applied Mathematics*, 13(1):259–277.

[19] Harten, A. (1983). On the symmetric form of systems of conservation laws with entropy. *Journal of Computational Physics*, 49(1):151 – 164.

[20] Koellermeier, J. and Torrilhon, M. (2017). Numerical study of partially conservative moment equations in kinetic theory. *Communications in Computational Physics*, 21(4):9811011.

[21] Levermore, C. D. (1996). Moment closure hierarchies for kinetic theories. *Journal of Statistical Physics*, 83(5):1021–1065.

[22] Mathis, H., Cancès, C., Godlewski, E., and Seguin, N. (2015). Dynamic model adaptation for multiscale simulation of hyperbolic systems with relaxation. *Journal of Scientific Computing*, 63(3):820–861.

[23] Mieussens, L. (2000). Discrete-velocity models and numerical schemes for the boltzmann-bgk equation in plane and axisymmetric geometries. *Journal of Computational Physics*, 162(2):429 – 466.

[24] Mueller, I. and Ruggeri, T. (1998). *Rational extended thermodynamics*. Springer, 67 edition.

[25] Nordstrom, J. (2016). A roadmap to well posed and stable problems in computational physics. *Journal of Scientific Computing*, pages 1–21.

[26] Nordstrom, J., Eriksson, S., and Eliasson, P. (2012). Weak and strong wall boundary procedures and convergence to steady-state of the Navier-Stokes equations. *Journal of Computational Physics*, 231(14):4867 – 4884.

[27] Nordstrom, J. and Svard, M. (2005). Well-posed boundary conditions for the Navier-Stokes equations. *SIAM Journal on Numerical Analysis*, 43(3):1231–1255.

[28] Rana, A. S. and Struchtrup, H. (2016). Thermodynamically admissible boundary conditions for the regularized 13 moment equations. *Physics of Fluids*, 28(2):027105.

[29] Rauch, J. B. and Massey, F. J. (1974). Differentiability of solutions to hyperbolic initial boundary value problems. *Transactions of the American Mathematical Society*, 189:303–318.

[30] Ringhofer, C., Schmeiser, C., and Zwirchmayr, A. (2001). Moment methods for the semiconductor Boltzmann equation on bounded position domains. *SIAM Journal on Numerical Analysis*, 39(3):1078–1095.

[31] Sarna, N. and Torrilhon, M. (2018). On stable wall boundary conditions for the hermite discretization of the linearised Boltzmann equation. *Journal of Statistical Physics*, 170(1):101–126.

[32] Struchtrup, H. (2008). What does an ideal wall look like? *Continuum Mechanics and Thermodynamics*, 19(8):493–498.

[33] Struchtrup, H. (2010). *Macroscopic Transport Equations for Rarefied Gas Flows*. Springer Ltd.

[34] Struchtrup, H., Beckmann, A., Rana, A. S., and Frezzotti, A. (2017). Evaporation boundary conditions for the r13 equations of rarefied gas dynamics. *Physics of Fluids*, 29(9):092004.

[35] Struchtrup, H. and Torrilhon, M. (2007). H-theorem, regularization, and boundary conditions for linearized 13 moment equations. *Phys. Rev. Lett.*, 99:014502.

[36] Svard, M. (2015). Weak solutions and convergent numerical schemes of modified compressible navier-stokes equations. *Journal of Computational Physics*, 288(Supplement C):19 – 51.

[37] Svard, M. and Ozcan, H. (2014). Entropy-stable schemes for the euler equations with far-field and wall boundary conditions. *Journal of Scientific Computing*, 58(1):61–89.

[38] Tadmor, E. (2003). Entropy stability theory for difference approximations of nonlinear conservation laws and related time-dependent problems. *Acta Numerica*, 12:451512.

[39] Torrilhon, M. (2015). Convergence Study of Moment Approximations for Boundary Value Problems of the Boltzmann-BGK Equation. *Communications in Computational Physics*, 18(03):529–557.

[40] Torrilhon, M., Au, J. D., and Struchtrup, H. (2003). Explicit fluxes and productions for large systems of the moment method based on extended thermodynamics. *Continuum Mechanics and Thermodynamics*, 15(1):97–111.

[41] Torrilhon, M. and Sarna, N. (2017). Hierarchical Boltzmann simulations and model error estimation. *Journal of Computational Physics*, 342:66 – 84.